

Strong, weak or no balance? Testing structural hypotheses against real networks

Anna Gallo,^{1,2} Diego Garlaschelli,^{1,2,3} Renaud Lambiotte,⁴ Fabio Saracco,^{5,6,1} and Tiziano Squartini^{1,2,7}

¹*IMT School for Advanced Studies, Piazza San Francesco 19, 55100 Lucca (Italy)*

²*INdAM-GNAMPA Istituto Nazionale di Alta Matematica (Italy)*

³*Lorentz Institute for Theoretical Physics, University of Leiden,
Niels Bohrweg 2, 2333 CA Leiden (The Netherlands)*

⁴*Mathematical Institute, University of Oxford, Woodstock Road, OX2 6GG Oxford (United Kingdom)*

⁵*‘Enrico Fermi’ Research Center (CREF), Via Panisperna 89A, 00184 Rome (Italy)*

⁶*Institute for Applied Computing ‘Mauro Picone’ (IAC),
National Research Council, Via dei Taurini 19, 00185 Rome (Italy)*

⁷*Institute for Advanced Study, University of Amsterdam,
Oude Turfmarkt 145, 1012 GC Amsterdam (The Netherlands)*

(Dated: June 16, 2023)

The abundance of data about social, economic and political relationships allows social theories to be tested against empirical evidence and human behaviour to be analyzed just as any other natural phenomenon. Here we focus on balance theory, stating that actors in signed social networks tend to avoid the formation of ‘unbalanced’, or ‘frustrated’, cycles, i.e. cycles with an odd number of negative links. This statement can be supported statistically only after a comparison with a null model. Since the existing benchmarks do not typically account for the heterogeneity of individual actors, here we first extend the Exponential Random Graphs framework to signed networks with both global (homogeneous) and local (heterogeneous) constraints and then employ them to assess the significance of unbalanced patterns in several real-world networks. We find that the nature and level of balance in social networks crucially depends on the null model employed. In particular, the study of signed triangles and signed communities reveals that homogeneous null models favour the weak version of balance theory, according to which only triangles with one negative link should be under-represented in social networks, while heterogeneous null models favour the strong version of balance theory, according to which also triangles with all negative links should be under-represented. Biological networks, instead, display almost inverted patterns and strong frustration under any benchmark, confirming that structural balance inherently distinguishes social networks from other signed networks.

PACS numbers: 89.75.Fb; 89.65.-s; 02.50.Tt

Network theory has emerged as a powerful framework in many disciplines to model different kinds of real-world systems, by representing their units as *nodes* and the interactions between them as *links*. In social science, the study of networks with *signed edges* has recently seen its popularity revived [1–4], because the signed character of links can be used to represent the positive as well as the negative social interactions that are currently identifiable in empirical data.

From a historical perspective, the interest in the study of signed networks is rooted into the so-called *balance theory* (BT), firstly proposed by Heider [5] and further developed by Cartwright and Harary [6]. The choice of adopting signed graphs to model BT led to the introduction of the so-called *structural balance theory* [6] which has found application not only in the study of human relationships but also in that of biological, ecological and economic systems [7–10].

BT deals with the concept of *balance*: a complete, signed graph is said to be balanced if all its triads have an even number of negative edges, i.e. either zero (in this case, the three edges are all positive) or two (see Fig. 1). Informally speaking, BT formalizes the principles ‘the friend of my friend is my friend’ and ‘the enemy of my enemy

is my friend’. The so-called *structure theorem* states that a complete, signed graph is balanced if and only if its set of nodes can be partitioned into two, disjoint subsets whose intra-modular links are all positive and whose inter-modular links are all negative. Cartwright and Harary extended the definition of balance to incomplete graphs [6] by including cycles of length larger than three: a (connected) network is said to be balanced when *all* cycles are positive, i.e. they contain an even number of negative edges. Taken together, the criteria above form the so-called *strong balance theory* (SBT).

The framework of SBT has been extended by Davis [11] by introducing the concept of *k-balanced* networks, according which signed graphs are balanced if their set of nodes can be partitioned into *k* disjoint subsets with positive intra-modular links and negative inter-modular links. This generalized definition of balance leads to the formulation of *weak balance theory* (WBT), according to which triads with all negative edges are balanced, since each of their nodes can be thought of as a group on its own if necessary (see Fig. 1).

Several metrics to decide whether signed networks are strongly or weakly balanced have been proposed. For instance, the degree of balance of a signed network has been

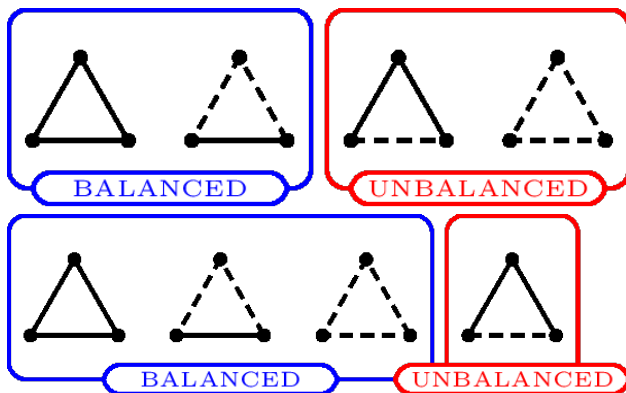


FIG. 1: Fundamental triadic patterns, or motifs, considered as balanced (blue) and unbalanced (red) by the strong (top) and weak (bottom) versions of balance theory.

quantified as the number of edges that need be removed, or whose sign need be reversed, in order to obtain a network where each cycle has an even number of negative links [12, 13]. Alternatively, it has been defined as the number of balanced, closed walks (i.e. closed walks with an even number of negative links) that are present in the network [14–17]. In [18] an incomplete, signed network is considered balanced if it is possible to fill in all its missing links to obtain a complete, balanced graph according to SBT. In [19] the authors define three different levels of balance: at the micro-scale, involving triads; at the meso-scale, involving larger subgraphs; and at the macro-scale, involving the entire network. Other approaches have been adopted in [20–22], where the problem is studied from a spectral perspective, and in [23], where the problem is studied by employing concepts borrowed from statistical physics (each signed triad is assigned an energy and the networks at the ‘lowest temperature’ have triangles without negative edges).

Other authors, instead, have focused on the complementary notion of *frustration*, trying to quantify the extent to which signed networks are far from balanced [19, 24–26]. In [24], the authors define the so-called *balanced decomposition number*, i.e. the (minimum) number of balanced groups into which nodes can be partitioned, and evaluate it by counting the (minimum) number of edges whose removal increases a network balance. In [27], instead, the same index is evaluated by adopting the so-called *switching signs method* introduced in [28] and prescribing to count the (minimum) number of signs that must be reversed to balance a network. In [20], the degree of (im)balance of a network is proxied by the magnitude of the smallest eigenvalue of the Laplacian matrix.

Empirical observations seem to point out that real-world, signed networks tend to be k -balanced, i.e. to avoid establishing the patterns that are considered as frustrated by WBT: as an example, in [22] the authors

study a pair of online, social networks induced by the relationships between users, showing that balance increases as the number of clusters into which nodes are partitioned is larger than two. In [17], the authors notice that the weak formulation of BT allows a better performance in predicting signs to be achieved.

In the present paper, we concentrate on the fact that any measure of balance (or frustration) is not meaningful by itself: in order to perform a statistically sound analysis, its empirical value must be compared with the outcome of a properly defined benchmark model, i.e. a reference model preserving some of the network properties while randomizing the rest. The most common null model for signed graphs is perhaps the one obtained by keeping the positions of edges fixed while shuffling their signs [2, 17]. Ref. [29] implements what we may call (for reasons that will be clear later) the *canonical* variant of the aforementioned exercise, assigning signs by means of a Bernoulli distribution. Ref. [15] introduces a null model for randomizing both the presence and the sign of links. In [10], the signed version of the Local Rewiring Algorithm is implemented (at each step, two edges with the same sign are selected and rewired, to preserve the total number of signed links incident to each node). The canonical variant of this model is implemented in [30], where the Balanced Signed Chung-Lu model (BSCL) is proposed (although it additionally constrains also the average number of signed triangles each edge is part of). Finally, refs. [31–34] define models constraining the structural properties of signed networks within the framework of Exponential Random Graphs (ERG).

Our contribution here focuses on binary, undirected signed networks and is motivated by two key considerations. First, real-world social networks have different levels of sparsity and we therefore aim at extending the ERG framework to include null models suitable for the analysis of signed graphs with ‘plus’ (positive), ‘minus’ (negative) and additionally ‘zero’ (missing) edges. Second, as in the analysis of most other networks, we recognize the importance of preserving the inherent heterogeneity of different nodes and we therefore define new null models that can constrain the number of plus, minus and zero edges of each node separately. As we shall see, controlling for the different tendencies of actors of establishing friendly and unfriendly relationships can change the estimated statistical significance of balance quite dramatically. After defining a suite of such null models, we will use them to inspect the statistical significance of the most commonly studied (un)balanced patterns at both local and global levels, i.e. signed triangles and signed communities.

FORMALISM AND BASIC QUANTITIES

A *signed* graph is a graph where each edge can be *positive*, *negative* or *missing*. In what follows, we will focus

on binary, undirected, signed networks: hence, each edge will be ‘plus one’, ‘minus one’ or ‘zero’. More formally, for any two nodes i and j , the corresponding entry of the signed adjacency matrix \mathbf{A} will be assumed to be $a_{ij} = -1, 0, +1$ (with $a_{ij} = a_{ji}, \forall i < j$). Since the total number of node pairs is $\frac{N(N-1)}{2} = \binom{N}{2}$ and any node pair can be positively connected, negatively connected or disconnected, the total number of possible graph configurations is $|\mathbb{A}| = 3^{\binom{N}{2}}$. To ease mathematical manipulations, let us define the following three quantities:

$$a_{ij}^- = [a_{ij} = -1], \quad a_{ij}^0 = [a_{ij} = 0], \quad a_{ij}^+ = [a_{ij} = +1] \quad (1)$$

where we have employed Iverson’s brackets notation (see Appendix A). These new variables are mutually exclusive, i.e. $\{a_{ij}^-, a_{ij}^0, a_{ij}^+\} = \{(1, 0, 0), (0, 1, 0), (0, 0, 1)\}$, sum to 1, i.e. $a_{ij}^- + a_{ij}^0 + a_{ij}^+ = 1$, and induce two non-negative matrices $\mathbf{A}^+, \mathbf{A}^-$ such that $\mathbf{A} = \mathbf{A}^+ - \mathbf{A}^-$ and $|\mathbf{A}| = \mathbf{A}^+ + \mathbf{A}^-$.

The numbers of positive and negative links are defined as

$$L^+ = \sum_{i=1}^N \sum_{j<i} a_{ij}^+ \quad \text{and} \quad L^- = \sum_{i=1}^N \sum_{j<i} a_{ij}^-. \quad (2)$$

Analogously, the positive and negative degrees of node i are

$$k_i^+ = \sum_{j<i} a_{ij}^+ \quad \text{and} \quad k_i^- = \sum_{j<i} a_{ij}^- \quad (3)$$

(naturally, $2L^+ = \sum_{i=1}^N k_i^+$ and $2L^- = \sum_{i=1}^N k_i^-$). The advantage of adopting Iverson’s brackets is that each quantity is now computed from a matrix with positive entries, so that all quantities of interest are positive as well.

Let us now focus on the signed triads (see Fig. 2), which represent one of the starting points to verify the strong and weak versions of BT. As mentioned above, according to BT social systems tend to arrange themselves into configurations satisfying the principles ‘the friend of my friend is my friend’, ‘the friend of my enemy is my enemy’, ‘the enemy of my friend is my enemy’, ‘the enemy of my enemy is my friend’ [5]. SBT formalizes this concept by stating that the overall network balance increases with the fraction of triangles having an even number of negative edges (said to be balanced or ‘positive’ since the product of the edge signs is a ‘plus’) and decreases with the fraction of triangles having an odd number of negative edges (said to be unbalanced or ‘negative’ since the product of the edge signs is a ‘minus’). WBT, on the other hand, considers the triangle with all negative edges balanced as well.

Notice that the product of an arbitrary number of matrices of type \mathbf{A}^+ and \mathbf{A}^- allows us to count the abundance of closed walks whose signature matches the sequence of signs of the matrices. For example, the expression $[\mathbf{A}^+ \mathbf{A}^- \mathbf{A}^+]_{ii}$ counts the number of closed walks, starting from and ending at i , of length 3 and signature $(+ - +)$. Similarly, the expression $[\mathbf{A}^+ \mathbf{A}^+ \mathbf{A}^- \mathbf{A}^+]_{ii} = [(\mathbf{A}^+)^2 \mathbf{A}^- \mathbf{A}^+]_{ii}$ counts the number of closed walks, starting from and ending at i , of length 4 and signature $(+ + - +)$. Therefore, the degree of balance of a network can be quantified by the abundance of (non-degenerate) triangles with an even number of negative links, i.e.

$$T^{(+++)} = \frac{1}{3} \sum_{i=1}^N T_i^{(+++)} = \frac{\text{Tr}[(\mathbf{A}^+)^3]}{6}, \quad (4)$$

$$T^{(+-+)} = \frac{1}{2} \sum_{i=1}^N T_i^{(+-+)} = \frac{\text{Tr}[\mathbf{A}^+ (\mathbf{A}^-)^2]}{2}. \quad (5)$$

Similarly, the degree of frustration of a network can be quantified by the abundance of (non-degenerate) triangles with an odd number of negative links, i.e.

$$T^{(---)} = \frac{1}{3} \sum_{i=1}^N T_i^{(---)} = \frac{\text{Tr}[(\mathbf{A}^-)^3]}{6}, \quad (6)$$

$$T^{(++-)} = \frac{1}{2} \sum_{i=1}^N T_i^{(++-)} = \frac{\text{Tr}[(\mathbf{A}^+)^2 \mathbf{A}^-]}{2} \quad (7)$$

(see Appendix B for more details).

The above expressions form the basis for the definition of several indices quantifying the degree of balance of a network. For instance, the total number of balanced patterns according to SBT is $\#_{\Delta}^{sb} = T^{(+++)} + T^{(+-+)}$, while the total number of unbalanced patterns is $\#_{\Delta}^{su} = T^{(---)} + T^{(++-)}$. Hence, we may naturally define a ‘strong balance index’ (SBI) and a corresponding ‘strong frustration index’ (SFI) as

$$\text{SBI} = \frac{\#_{\Delta}^{sb}}{\#_{\Delta}^{sb} + \#_{\Delta}^{su}}, \quad \text{SFI} = 1 - \text{SBI}. \quad (8)$$

On the other hand, the total number of balanced patterns according to WBT is $\#_{\Delta}^{wb} = T^{(+++)} + T^{(+-+)} + T^{(---)}$, while the total number of unbalanced patterns is $\#_{\Delta}^{wu} = T^{(++-)}$. Hence, we can introduce a ‘weak balance index’ (WBI) and a corresponding ‘weak frustration index’ (WFI) as

$$\text{WBI} = \frac{\#_{\Delta}^{wb}}{\#_{\Delta}^{wb} + \#_{\Delta}^{wu}}, \quad \text{WFI} = 1 - \text{WBI}. \quad (9)$$

The indices defined above quantify ‘imbalance’ by counting the abundance of locally frustrated, short cycles. Other indices of frustration account for higher-order

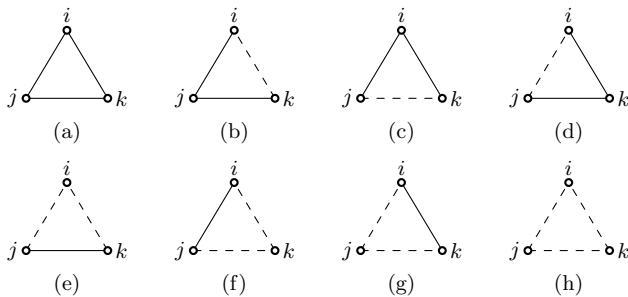


FIG. 2: Signed triangles involving three representative nodes i, j, k . Solid lines denote positive edges while dashed lines denote negative edges. According to the strong version of balance theory, triangles (a), (e), (f) and (g) are balanced, while triangles (b), (c), (d) and (h) are unbalanced. According to the weak version, triangles (a), (e), (f), (g) and (h) are balanced, while triangles (b), (c) and (d) are unbalanced.

structures that may result from the effects of structural (im)balance at larger scales. In particular, at the mesoscopic level, the effect of structural balance would result in a signed network being partitioned into communities of nodes, where intra-community links would be preferentially positive and inter-community links would be preferentially negative. Correspondingly, one can define a ‘higher-order frustration index’

$$\text{HOFI} = \frac{L_{\circ}^{+} + L_{\bullet}^{-}}{L} \quad (10)$$

measuring the percentage of ‘misplaced’ links, i.e. the total number L_{\circ}^{+} of positive links between communities, plus the total number L_{\bullet}^{-} of negative links within communities, divided by the total number L of links (the formalism is adapted from the one in [35]). According to SBT, the node partition minimizing frustration (and correspondingly the HOFI) should be the one corresponding to only two communities, because such bipartition can be realized without creating all-negative triangles. By contrast, WBT allows for a larger number of communities, because the theory justifies the presence of all-negative triangles precisely by assuming that the three participating nodes are all placed in different communities.

NULL MODELS OF BINARY, UNDIRECTED, SIGNED GRAPHS

Here we generalize the ERG framework to account for models of binary, undirected, signed graphs. We will follow the analytical approach introduced in [36], and further developed in [37], aimed at identifying the functional form of the maximum-entropy probability distribution (over all graphs of a chosen type) that preserves

a desired set of empirical constraints on average. Specifically, this approach looks for the graph probability $P(\mathbf{A})$ that maximizes Shannon entropy

$$S = - \sum_{\mathbf{A} \in \mathbb{A}} P(\mathbf{A}) \ln P(\mathbf{A}) \quad (11)$$

(where the sum runs over the set \mathbb{A} , of cardinality $|\mathbb{A}| = 3^{\binom{N}{2}}$, of all binary, undirected, signed graphs) under a set of constraints enforcing the expected value of a chosen set of properties. The formal solution to this problem is the exponential probability $P(\mathbf{A}) = e^{-H(\mathbf{A})}/Z$ where $H(\mathbf{A})$ (the *Hamiltonian*) is a linear combination of the constrained properties, each multiplied by a corresponding Lagrange multiplier, and $Z = \sum_{\mathbf{A} \in \mathbb{A}} e^{-H(\mathbf{A})}$ is the normalizing constant (or *partition function*).

In what follows, we will consider two classes of models, i.e. those keeping the network topology fixed and those letting the topology vary along with the edge signs. The first class is better suited for studying systems where actors cannot choose ‘with whom’ to interact, but only ‘how’ (e.g. because workers necessarily interact with colleagues at the same workplace or because countries necessarily interact with each other). On the other hand, the second class is better suited for studying systems where actors can choose their neighbours as well [17]. Whatever the situation, comparing the two types of models for the same network is in any case instructive, as it allows the role played by signed constraints to be disentangled from the one played by non-signed (purely topological) constraints.

A summary of the null models introduced in the rest of this section is provided in Table I.

Signed Random Graph Model

As the simplest example, the Signed Random Graph Model (SRGM) is defined by two, global constraints: $L^{+}(\mathbf{A})$ and $L^{-}(\mathbf{A})$. The Hamiltonian

$$H(\mathbf{A}) = \alpha L^{+}(\mathbf{A}) + \beta L^{-}(\mathbf{A}) \quad (12)$$

leads to a graph probability $P_{\text{SRGM}}(\mathbf{A})$ that factorizes over the individual entries of the matrix \mathbf{A} , which are i.i.d. random variables described by the finite scheme

$$a_{ij} \sim \begin{pmatrix} -1 & 0 & +1 \\ p^{-} & p^{0} & p^{+} \end{pmatrix} \quad \forall i < j \quad (13)$$

with $p^{0} \equiv 1 - p^{-} - p^{+}$ and

$$p^{-} \equiv \frac{e^{-\beta}}{1 + e^{-\alpha} + e^{-\beta}} \equiv \frac{y}{1 + x + y}, \quad (14)$$

$$p^{+} \equiv \frac{e^{-\alpha}}{1 + e^{-\alpha} + e^{-\beta}} \equiv \frac{x}{1 + x + y}, \quad (15)$$

	Topology: free	Topology: fixed
Homogenous	SRGM: each pair of nodes is assigned a ‘plus’, a ‘minus’ or a ‘zero’ edge with a probability that is pair-independent; all nodes are statistically equivalent. Differently from the recipe adopted in [15, 38], the parameters defining our SRGM can be unambiguously tuned to reproduce the empirical number of ‘plus’ and ‘minus’ edges of any (binary, undirected, signed) network.	SRGM-FT: the topology is the same as in the real network and the connected pairs of nodes are assigned either a ‘plus one’ or a ‘minus one’, with a probability that is pair-independent. Differently from the recipe adopted in [2, 29], the parameters defining our SRGM-FT can be unambiguously tuned to reproduce the empirical number of ‘plus’ and ‘minus’ edges of any (binary, undirected, signed) network. The SRGM-FT is the conditional version of the SRGM.
Heterogenous	SCM: each pair of nodes is assigned a ‘plus’, a ‘minus’ or a ‘zero’ edge, with a probability that is pair-dependent and determined by the different tendencies of nodes to establish positive and negative interactions. This model represents the canonical variant of the one employed in [10].	SCM-FT: the topology is the same as in the real network and the connected pairs of nodes are assigned either a ‘plus one’ or a ‘minus one’, with a probability that is pair-dependent and determined by the different tendencies of nodes to establish positive and negative interactions. The SCM-FT is the conditional version of the SCM.

TABLE I: Table summarizing the properties of the null models derived in this article for the first time.

where $x \equiv e^{-\alpha}$ and $y \equiv e^{-\beta}$ are transformed Lagrange multipliers (see Appendix C for more details). In other words, positive, negative and missing links appear with probability p^+ , p^- and p^0 respectively. The parameters (x, y) determining these probabilities are tuned by maximizing the log-likelihood function $\mathcal{L}_{\text{SRGM}}(x, y) \equiv \ln P_{\text{SRGM}}(\mathbf{A}^*|x, y)$ where \mathbf{A}^* denotes the specific, empirical network under analysis. This maximization, according to a general result [39], leads to an equality between the expected and the empirical values of the constraints, i.e. $\langle L^+ \rangle_{\text{SRGM}} = L^+(\mathbf{A}^*)$ and $\langle L^- \rangle_{\text{SRGM}} = L^-(\mathbf{A}^*)$. This leads to $p^0 \equiv 1 - p^- - p^+$ and

$$p^+ = \frac{2L^+(\mathbf{A}^*)}{N(N-1)}, \quad p^- = \frac{2L^-(\mathbf{A}^*)}{N(N-1)}. \quad (16)$$

Signed Random Graph Model with Fixed Topology

We can also consider a variant of the SRGM that keeps the topology of the network under analysis fixed while (solely) randomizing the edge signs. The Hamiltonian is again $H(\mathbf{A}) = \alpha L^+(\mathbf{A}) + \beta L^-(\mathbf{A})$, but the random variables are now only the entries of the adjacency matrix corresponding to the connected pairs of nodes in the original network \mathbf{A}^* , i.e. the ones for which $|a_{ij}^*| = 1$. These entries obey the finite scheme

$$a_{ij} \sim \begin{pmatrix} -1 & +1 \\ p^- & p^+ \end{pmatrix} \quad \forall i < j \mid |a_{ij}^*| = 1 \quad (17)$$

with

$$p^- \equiv \frac{e^{-\beta}}{e^{-\alpha} + e^{-\beta}} \equiv \frac{y}{x + y}, \quad (18)$$

$$p^+ \equiv \frac{e^{-\alpha}}{e^{-\alpha} + e^{-\beta}} \equiv \frac{x}{x + y}. \quad (19)$$

In other words, each entry for which $|a_{ij}^*| = 1$ obeys a Bernoulli distribution with probabilities determined by the (Lagrange multipliers of the) imposed constraints (see Appendix C for more details). The maximization of the likelihood function $\mathcal{L}_{\text{SRGM-FT}}(x, y) \equiv \ln P_{\text{SRGM-FT}}(\mathbf{A}^*|x, y)$ (where FT stands for ‘fixed topology’) leads to

$$p^+ = \frac{L^+(\mathbf{A}^*)}{L(\mathbf{A}^*)}, \quad p^- = \frac{L^-(\mathbf{A}^*)}{L(\mathbf{A}^*)} \quad (20)$$

with $L(\mathbf{A}^*)$ representing the (empirical) number of links.

Remarkably, the SRGM and the SRGM-FT are related via the simple expression

$$P_{\text{SRGM}}(\mathbf{A}) = P_{\text{RGM}}(\mathbf{A}) \cdot P_{\text{SRGM-FT}}(\mathbf{A}) \quad (21)$$

involving the probability of the usual ‘unsigned’ (Erdős-Rényi) Random Graph Model (RGM) and stating that the probability of connecting any two nodes with, say, a positive link can be rewritten as the probability of connecting them with an unsigned link times the probability of assigning the latter a ‘plus one’: in formulas, $p_{\text{SRGM}}^+/p_{\text{RGM}} = p_{\text{SRGM-FT}}^+$ (see Appendix C for more details). Notice that if the network under analysis is completely connected, the SRGM and the SRGM-FT coincide.

Although the recipes implemented in [15] and [2, 29] are similar in spirit to the SRGM and the SRGM-FT, the rigorous derivation of both models is provided here for the first time, together with the proof that the latter is nothing but the conditional version of the former.

Signed Configuration Model

The two aforementioned versions of the SRGM are defined by constraints which are global in nature. However, real social networks are characterized by an inherent heterogeneity of actors, which results in broad distributions of the number of connections of actors. To avoid statistical conclusions about structural balance that are biased by the application of homogeneous null models to intrinsically heterogeneous networks, it is therefore important to introduce models with local (node-specific) constraints.

We therefore introduce the Signed Configuration Model (SCM) via the Hamiltonian

$$H(\mathbf{A}) = \sum_{i=1}^N [\alpha_i k_i^+(\mathbf{A}) + \beta_i k_i^-(\mathbf{A})] \quad (22)$$

which constraints the expected value of the signed degrees $\{k_i^+(\mathbf{A})\}_{i=1}^N$ and $\{k_i^-(\mathbf{A})\}_{i=1}^N$ of all nodes. The resulting graph probability $P_{\text{SCM}}(\mathbf{A})$ is still factorized over independent entries of the matrix \mathbf{A} , however these entries are no longer identically distributed. Rather, they obey the finite scheme

$$a_{ij} \sim \begin{pmatrix} -1 & 0 & +1 \\ p_{ij}^- & p_{ij}^0 & p_{ij}^+ \end{pmatrix} \quad \forall i < j \quad (23)$$

with

$$p_{ij}^- \equiv \frac{e^{-(\beta_i + \beta_j)}}{1 + e^{-(\alpha_i + \alpha_j)} + e^{-(\beta_i + \beta_j)}} \equiv \frac{y_i y_j}{1 + x_i x_j + y_i y_j}, \quad (24)$$

$$p_{ij}^+ \equiv \frac{e^{-(\alpha_i + \alpha_j)}}{1 + e^{-(\alpha_i + \alpha_j)} + e^{-(\beta_i + \beta_j)}} \equiv \frac{x_i x_j}{1 + x_i x_j + y_i y_j} \quad (25)$$

and $p_{ij}^0 \equiv 1 - p_{ij}^- - p_{ij}^+$ (see Appendix C for more details). In other words, the two nodes i and j are connected by a positive, negative or missing link with probability p_{ij}^+ , p_{ij}^- or p_{ij}^0 respectively. The parameters of the SCM are found by maximizing the log-likelihood $\mathcal{L}_{\text{SCM}}(\{x_i\}_{i=1}^N, \{y_i\}_{i=1}^N) \equiv \ln P_{\text{SCM}}(\mathbf{A}^* | \{x_i\}_{i=1}^N, \{y_i\}_{i=1}^N)$, and the result ensures that $\langle k_i^+ \rangle_{\text{SCM}} = k_i^+(\mathbf{A}^*)$ and $\langle k_i^- \rangle_{\text{SCM}} = k_i^-(\mathbf{A}^*)$, $\forall i$. Explicitly,

$$k_i^+(\mathbf{A}^*) = \sum_{j \neq i} \frac{x_i x_j}{1 + x_i x_j + y_i y_j} = \langle k_i^+ \rangle \quad \forall i, \quad (26)$$

$$k_i^-(\mathbf{A}^*) = \sum_{j \neq i} \frac{y_i y_j}{1 + x_i x_j + y_i y_j} = \langle k_i^- \rangle \quad \forall i, \quad (27)$$

which is a system of $2N$ coupled non-linear equations that have a unique solution to be found numerically, e.g.

following the guidelines provided in [40] (see Appendix D). If $x_i \ll 1$ and $y_i \ll 1 \forall i$, a ‘sparse’ approximation of the SCM holds true and one can factorize the probabilities as $p_{ij}^+ \simeq x_i x_j$ and $p_{ij}^- \simeq y_i y_j$, $\forall i < j$. Such a manipulation leads us to

$$p_{ij}^+ \simeq \frac{k_i^+(\mathbf{A}^*) k_j^+(\mathbf{A}^*)}{2L^+(\mathbf{A}^*)}, \quad p_{ij}^- \simeq \frac{k_i^-(\mathbf{A}^*) k_j^-(\mathbf{A}^*)}{2L^-(\mathbf{A}^*)}, \quad (28)$$

a result that we may call the Signed Chung-Lu Model (SCLM).

To the best of our knowledge, the canonical SCM described here has no precedents in the literature: Ref. [10] provides a microcanonical version of the model, while the variant considered in [30] is just an approximation of the full canonical model derived here. Interestingly, the bipartite version of the SCM can be recovered as a special case of the Bipartite Score Configuration Model, proposed in [33].

Signed Configuration Model with Fixed Topology

As for the SRGM, a variant of the SCM that keeps the topology of the network under analysis fixed while (solely) randomizing the signs of the edges can be defined. Again, the Hamiltonian reads $H(\mathbf{A}) = \sum_{i=1}^N [\alpha_i k_i^+(\mathbf{A}) + \beta_i k_i^-(\mathbf{A})]$ but the only random variables are those corresponding to the connected pairs of nodes in the empirical graph, i.e. the ones for which $|a_{ij}^*| = 1$. Each of them obeys the finite scheme

$$a_{ij} \sim \begin{pmatrix} -1 & +1 \\ p_{ij}^- & p_{ij}^+ \end{pmatrix} \quad \forall i < j \mid |a_{ij}^*| = 1 \quad (29)$$

with

$$p_{ij}^- \equiv \frac{e^{-(\beta_i + \beta_j)}}{e^{-(\alpha_i + \alpha_j)} + e^{-(\beta_i + \beta_j)}} \equiv \frac{y_i y_j}{x_i x_j + y_i y_j}, \quad (30)$$

$$p_{ij}^+ \equiv \frac{e^{-(\alpha_i + \alpha_j)}}{e^{-(\alpha_i + \alpha_j)} + e^{-(\beta_i + \beta_j)}} \equiv \frac{x_i x_j}{x_i x_j + y_i y_j}. \quad (31)$$

Maximizing the log-likelihood $\mathcal{L}_{\text{SCM-FT}}(\{x_i\}_{i=1}^N, \{y_i\}_{i=1}^N) \equiv \ln P_{\text{SCM-FT}}(\mathbf{A}^* | \{x_i\}_{i=1}^N, \{y_i\}_{i=1}^N)$ leads to the equations

$$k_i^+(\mathbf{A}^*) = \sum_{j \neq i} |a_{ij}^*| \frac{x_i x_j}{x_i x_j + y_i y_j} = \langle k_i^+ \rangle \quad \forall i, \quad (32)$$

$$k_i^-(\mathbf{A}^*) = \sum_{j \neq i} |a_{ij}^*| \frac{y_i y_j}{x_i x_j + y_i y_j} = \langle k_i^- \rangle \quad \forall i, \quad (33)$$

which can be solved numerically - again, along the guidelines provided in [40] (see Appendix D for more details).

Similarly to what has been observed for the SRGM and the SRGM-FT, the SCM and the SCM-FT are related via

$$P_{\text{SCM}}(\mathbf{A}) = P_{\text{ICM}}(\mathbf{A}) \cdot P_{\text{SCM-FT}}(\mathbf{A}), \quad (34)$$

an expression involving the probability of an ordinary (unsigned) ‘induced’ Configuration Model (ICM) with probabilities such that $(p_{ij}^+)_{\text{SCM}}/(p_{ij})_{\text{ICM}} = (p_{ij}^+)_{\text{SCM}}/[(p_{ij}^+)_{\text{SCM}} + (p_{ij}^-)_{\text{SCM}}] = (p_{ij}^+)_{\text{SCM-FT}}$, for any pair of nodes (see Appendix C). Notice that, if the network under consideration is completely connected, then the SCM and the SCM-FT coincide. Like the SCM, the SCM-FT is derived here for the first time.

RESULTS

We now employ our benchmarks to analyze various real-world networks. Although most of them represent social relationships, we have also considered biological data as a comparison to check for specific patterns characterizing social structures.

The first dataset is the so-called ‘Correlates of Wars’ (CoW) dataset [41]. It provides a picture of the international political relationships over the years 1946-1997 and consists of 13 snapshots of 4 years each. A positive edge between any two countries indicates an alliance, a political agreement or the membership to the same governmental organization. Conversely, a negative edge indicates that the two countries are enemies, have a political disagreement or are part of different, governmental organizations.

The second dataset collects information about the relationships among the $\simeq 300.000$ players of a massive multiplayer online game (MMOG) [42]. A positive edge between two players indicates a friendship, an alliance, or an economic relation. Conversely, a negative edge indicates the existence of an enmity, a conflict, or a fight. Since the network is directed, we have projected it onto an undirected signed graph by applying the following rules (which preserve the total number of nodes): $+1 \cdot +1 = +1$; $+1 \cdot -1 = -1 \cdot +1 = -1$; $-1 \cdot -1 = -1$; $+1 \cdot 0 = 0 \cdot +1 = +1$; $-1 \cdot 0 = 0 \cdot -1 = -1$.

The remaining datasets we consider are those collected in [43] and analyzed in [25]. These include three socio-political networks (SPNs): *N.G.H. Tribes*, *Senate US*, *Monastery*; two financial networks (FNs): *Bitcoin Alpha* and *Bitcoin OTC*; and three gene-regulatory networks (GRNs): *E. Coli*, *Macrophage*, *Epidermal Growth Factor Receptor*.

In the SPNs, *N.G.H. Tribes* collects data about New Guinean Highland Tribes (here, a positive/negative link denotes alliance/rivalry), *Monastery* corresponds to the last frame of Sampson’s data about the relationships between novices in a monastery [44] (here, a posi-

tive/negative link indicates a positive/negative interaction), and *Senate US* collects data about the members of the 108th US Senate Congress (here, a positive/negative link indicates trust/distrust or similar/dissimilar political opinions).

The FNs are ‘who-trust-whom’ networks of Bitcoin traders on an online platform: a positive/negative link indicates trust/distrust between users [45]. The networks representing the FNs are weighted, directed ones: hence, after having binarized them by replacing each positive (negative) weight with a +1 (−1), we have made them undirected by applying the same rules adopted for the MMOG dataset.

Lastly, in the GRNs each node represents a gene, with positive links indicating activating connections and negative links indicating inhibiting connections. Specifically, *E. Coli* collects data about a transcriptional network of the bacterium *Escherichia Coli*; *Macrophage* collects data about a blood cell that eliminates substances such as cancer cells, cellular debris and microbes; *Epidermal Growth Factor Receptor* collects data about the protein that is responsible for cell division and survival in epidermal tissues.

The vast majority of the networks considered here is characterized by a small link density $c = 2L/N(N-1)$ but a large fraction L^+/L of positive links. The density of the CoW network decreases over time from $\simeq 0.2$ to $\simeq 0.1$ and the percentage of positive links is roughly stationary around $\simeq 88\%$; on the other hand, the link density of the MMOG network is stationary around 0.003 and the percentage of positive links decreases from $\simeq 98\%$ to $\simeq 60\%$. The SPNs have the largest values of link density among the configurations in our basket, ranging from $\simeq 0.3$ to $\simeq 0.5$, and percentages of positive links ranging from $\simeq 50\%$ to $\simeq 75\%$. *Bitcoin Alpha* has a link density of $\simeq 0.002$ and a percentage of positive links of $\simeq 90\%$, while *Bitcoin OTC* has a link density of $\simeq 0.001$ and a percentage of positive links of $\simeq 85\%$. Lastly, the GRNs have a link density ranging from $\simeq 10^{-3}$ to $\simeq 10^{-2}$ and a percentage of positive links ranging from $\simeq 58\%$ to $\simeq 66\%$.

In order to test the validity of BT in its two formulations, we need to compare the empirical abundance of the balance and frustration indices defined in the previous sections with the corresponding expected values calculated under the null models we have introduced. To this aim, a very useful indicator is represented by the z -score $z_m = [N_m(\mathbf{A}^*) - \langle N_m \rangle] / \sigma[N_m]$, where $N_m(\mathbf{A}^*)$ is the number of occurrences of pattern m in the real network \mathbf{A}^* , $\langle N_m \rangle$ is the expected occurrence of the same pattern under the chosen null model and $\sigma[N_m] = \sqrt{\langle N_m^2 \rangle - \langle N_m \rangle^2}$ is the standard deviation of N_m under the same null model. z_m quantifies the number of standard deviations by which the empirical abundance of pattern m differs from the expected one. For instance, after checking for the Gaussianity of

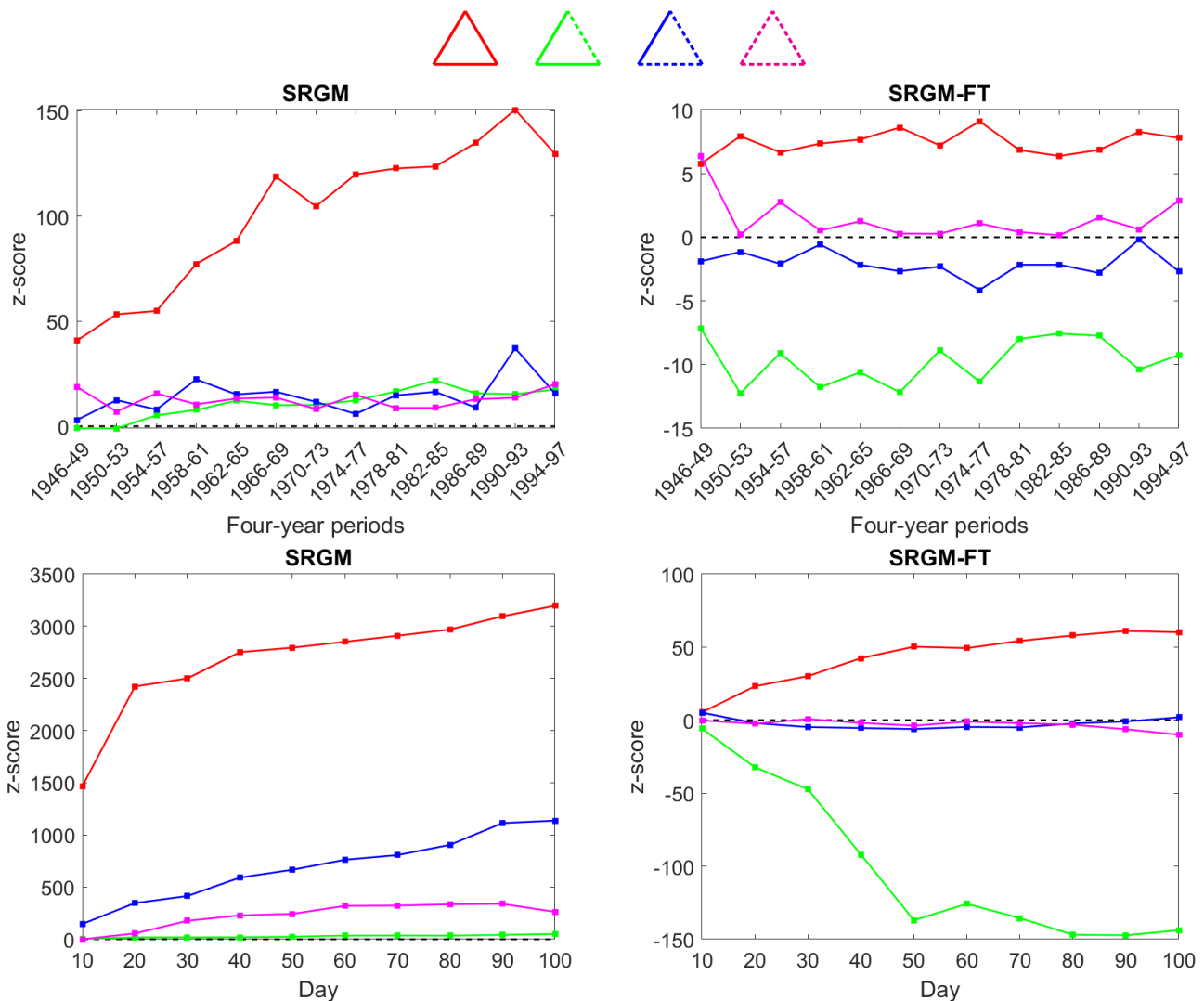


FIG. 3: Structural (im)balance in the CoW and MMOG datasets: evolution of the z -scores of signed triangles under homogeneous benchmarks (SRGM and SRGM-FT). Top panels refer to the 13 snapshots (of 4 years each) of the CoW dataset, covering the period 1946-1997. Bottom panels refer to the snapshots of the MMOG dataset. The SRGM-FT (right panels) supports WBT because the only significantly under-represented pattern in the data is also the only one that WBT considers frustrated (triangle with only one negative link), while the z -score of the triangle with all negative edges (which SBT would expect to be under-represented as well) is very low. In any case, the hypothesis that nodes tend to establish balanced triangles with all positive links is supported on both datasets. Results of this type constitute the backbone of the narrative according to which the weak version of BT is the one that is better supported by data. Note that the SRGM (left panels) has all z -scores positive, thereby not supporting any version of BT, a result due to the complete randomization of the topology along with the edge signs: the over-representation of all patterns in the data is merely due to the fact that triangles form with small probability at a purely topological level, given the low link density, irrespective of their signs.

N_m under the null model (which results from the fact that it is the sum of several almost independent random variables), a result $|z_m| \leq 2$ ($|z_m| \leq 3$) indicates that the empirical abundance of pattern m is compatible with the one expected under the chosen null model at the 5% (1%) level of statistical significance. On the other hand, a value $|z_m| > 2$ ($|z_m| > 3$) indicates that the empirical

abundance of pattern m is not compatible with the null model at those significance levels. In the latter case, a value $z_m > 0$ ($z_m < 0$) indicates the tendency of the pattern to be over- (under-)represented in the data with respect to the null model.

We can compute the z -scores by numerically sampling the ensembles of graphs defined by our null models. Since

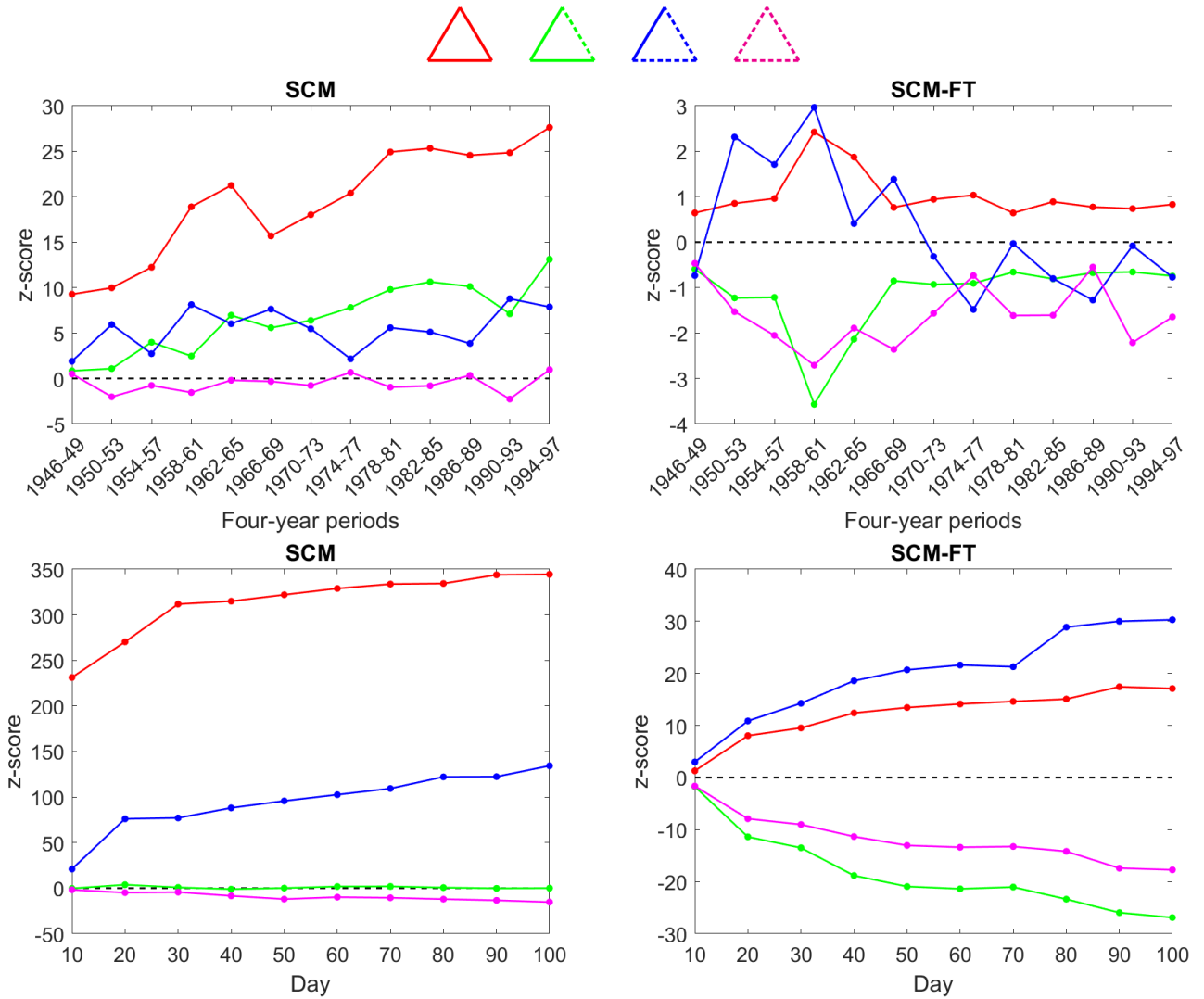


FIG. 4: Structural (im)balance in the CoW and MMOG datasets: evolution of the z -scores of signed triangles under heterogeneous benchmarks (SCM and SCM-FT). Top panels refer to the 13 snapshots (of 4 years each) of the CoW dataset, covering the period 1946-1997. Bottom panels refer to the snapshots of the MMOG dataset. The z -scores produced by the SCM (left panels) and the SCM-FT (right panels) are much smaller, in absolute value, than the corresponding ones produced by the SRGM and the SRGM-FT (see Fig. 3), showing that node heterogeneity contributes significantly to the overall abundance of signed triangles. The all-positive (balanced) triangle is still strongly over-represented in all cases, but additionally the all-negative (frustrated) triangle is now always under-represented. Under the SCM-FT, the other frustrated triangle (the one with a single negative link) is also systematically under-represented, and these combined results provide support for SBT (particularly evidently for the MMOG data). By contrast, WBT (according to which one would expect the under-representation of only the triangle with a single negative link) is no longer supported. These results provide an alternative narrative w.r.t. the usual one: when the heterogeneity of the signed degrees of nodes is accounted for, statistical evidence supports SBT rather than WBT.

the entries of the adjacency matrix are independent random variables, the unbiased generation of a random matrix $\mathbf{A} \in \mathbb{A}$ can be carried out by drawing a real number $u_{ij} \in U[0,1]$ and posing: for models with varying topology, $a_{ij} = -1$ if $0 \leq u_{ij} \leq p_{ij}^-$, $a_{ij} = +1$ if $p_{ij}^- < u_{ij} < p_{ij}^- + p_{ij}^+$ and $a_{ij} = 0$ if $p_{ij}^- + p_{ij}^+ \leq u_{ij} \leq 1$, for

all pairs $i < j$; for models with fixed topology, $a_{ij} = -1$ if $0 \leq u_{ij} \leq p_{ij}^-$ and $a_{ij} = +1$ if $p_{ij}^- < u_{ij} \leq 1$, for all pairs $i < j$ such that $|a_{ij}^*| = 1$.

We report our results starting from the network datasets that have several temporal snapshots (CoW and MMOG). Fig. 3 shows the temporal trends of the z -

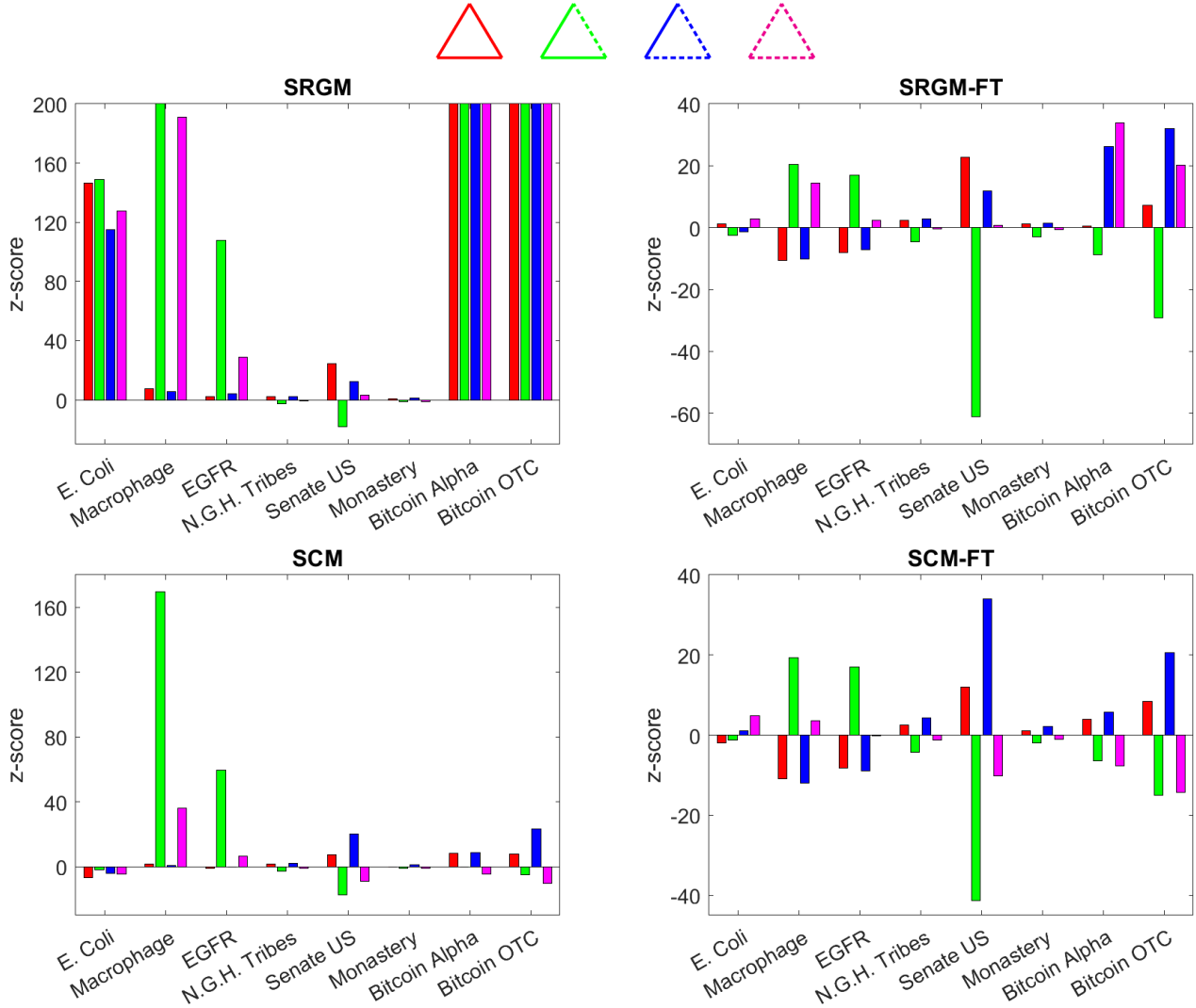


FIG. 5: Structural (im)balance in social and biological networks under homogeneous (top) and heterogeneous (bottom) null models: z -scores of signed triangles for three socio-political networks (*N.G.H. Tribes*, *Senate US*, *Monastery*), two financial networks (*Bitcoin Alpha*, *Bitcoin OTC*) and, as a comparison, three biological networks (*E. Coli*, *Macrophage*, *EGFR*). The SRGM produces z -scores that are almost always positive and very large for all triangles (balanced and unbalanced) and all signed networks (social and biological), a result confirming that this null model is completely uninformative about structural (im)balance, as it merely highlights that the formation of any triangle, irrespective of its signs, is highly unlikely if the topology is randomized completely. By contrast, the SRGM-FT largely supports WBT on social networks, as the only pattern under-represented in the data is the frustrated triangle with a single negative link. Heterogeneous null models (SCM and SCM-FT), instead, systematically support SBT because they assign positive z -scores to the two balanced triangles (all-positive and with two negative links) and negative z -scores to the two frustrated triangles (all-negative and with one negative link). Additionally, in biological networks they tend to assign opposite signs (w.r.t. social networks) to most z -scores, highlight a strong tendency towards imbalance. These results are fully in line with what already observed with the CoW and MMOG datasets in Figs. 3 and 4.

scores for the two networks under the homogeneous null models (SRGM and SRGM-FT). The panels on the left refer to the SRGM and show that the z -scores for all triangles, irrespective of their signs, are strong and positive. This means that all triangles are over-represented in the

data, with respect to a null model that completely randomizes the topology. This result is not unexpected, as it merely indicates that, given the empirical density of links, it is very unlikely to form triangles completely by chance. These results simply tell us that the SRGM is

uninformative about the (im)balance in the data, as it is entirely biased by a purely topological effect. This conclusion is in line with the results in [17], which suggested that the SRGM-FT is to be preferred over the SRGM as it provides a better explanation of empirical network structures.

By contrast, the results generated under the SRGM-FT (right panels) clearly support WBT. Indeed, the only significantly over-represented pattern in the data is precisely the only one that WBT considers frustrated (the triangle with a single negative link), whereas the empirical abundance of the triangle with all negative edges (which SBT would predict to be over-represented as well) remains largely compatible with the null model. Interestingly, also the empirical abundance of the balanced triangle with two negative edges is close to the one expected under the SRGM-FT, although its z -score is typically smaller than the z -score of the all-negative triangle. In any case, the abundance of the balanced triangle with three positive edges is significantly over-represented on both datasets. This type of results constitute the backbone of the narrative according to which the weak version of BT is the one that is better supported by data [2, 17].

However, since both the SRGM and the SRGM-FT do not constrain the local (node-specific) signed properties (i.e. the signed degrees of nodes), they cannot disentangle the effects of node heterogeneity from the revealed overall structural (im)balance. For this reason, in Fig. 4 we repeat the analysis of the CoW and MMOG datasets using the SCM and SCM-FT null models. As expected, the resulting z -scores are much smaller in absolute value, showing that node heterogeneity in the real networks is in general strong and is responsible for a significant part of the overall measured (im)balance. Therefore, controlling for the local signed degrees is a way to filter out the effects of node heterogeneity in the statistical analysis of structural balance. In general, we see that the triangle with all negative links has now negative z -scores in both datasets, under both null models. Similarly, the all-positive triangle remains with positive z -scores in all cases. The level of statistical significance (i.e. the absolute value of the z -score) is however quite different in the various cases: in general we see an overwhelming over-representation of the two balanced triangles (the all-positive one and the one with two negative links) in the MMOG data under both null models, while for the CoW data the only clearly significant pattern is the over-representation of the all-positive triangle in the SCM. Nicely, the SCM-FT gives always negative z -scores to both the frustrated triangles (the all-negative one and the one with only one negative link), and most of the time positive z -scores to the two balanced triangles. Although the statistical evidence is much stronger for the MMOG data, this result indicates that, if any, the version of BT supported by the data is SBT, rather than WBT. Therefore, as soon as the heterogeneity of the signed degrees of nodes is accounted for,

WBT loses its statistical support, and SBT is favoured by the data.

We now move to the results obtained on datasets which include other social networks as well as various biological networks, providing a different real-world benchmark where structural balance theory is not expected to apply. From Fig. 5 we confirm that the SRGM is completely uninformative about structural (im)balance, as it produces z -scores that are typically positive and very large for all triangles (balanced and unbalanced) and all networks (social and biological). This result simply means that the formation of any triangle, irrespective of its defining signs, is highly unlikely if the topology is completely randomized. By contrast, under the SRGM-FT the only pattern that is under-represented in social network data is the frustrated triangle with a single negative link, a result that largely supports WBT (on biological data, this pattern is instead either not significant or over-represented). Heterogeneous null models (SCM and SCM-FT), instead, assign positive z -scores to the two balanced triangles (all-positive and with two negative links) and negative z -scores to the two frustrated triangles (all-negative and with one negative link), thereby systematically supporting SBT. When used on biological networks, they instead highlight a strong tendency towards imbalance, as they tend to assign opposite signs (w.r.t. social networks) to most z -scores. These results confirm and extend what discussed above for the CoW and MMOG datasets, and additionally show that biological networks behave very differently from social networks, somehow favouring frustration. This is an indication that structural balance is indeed an inherent property of social networks.

As further evidence supporting the above conclusion, in Fig. 6 we show, for all networks and under all null models, the z -scores of the frustration indices SFI and WFI defined in Eqs. 8 and 9 respectively. Note that, while the raw values of SFI and WFI would not discount the effects of the imposed structural constraints on the raw values of frustration, the z -scores measure the level of statistical significance of the ‘residual’ frustration, after the structural constraints are accounted for. We see that, under all null models, the z -scores (when significant) are always negative for the social networks (signalling under-representation of the frustration indices in the data) and always positive for the biological networks (signalling over-representation of frustration in the data). Moreover, for the models with fixed topology, the z -scores for the heterogeneous null model (SCM-FT) are systematically smaller (in absolute value) than the ones for the corresponding homogeneous model (SRG-FT), indicating that, compared with the latter, the former model ‘explains more’ of the level of empirical frustration observed in the data. The same relation does not apply systematically between the models with varying topology (SCM and SRG), suggesting that models with fixed topology lead to more robust conclusions, as already ob-

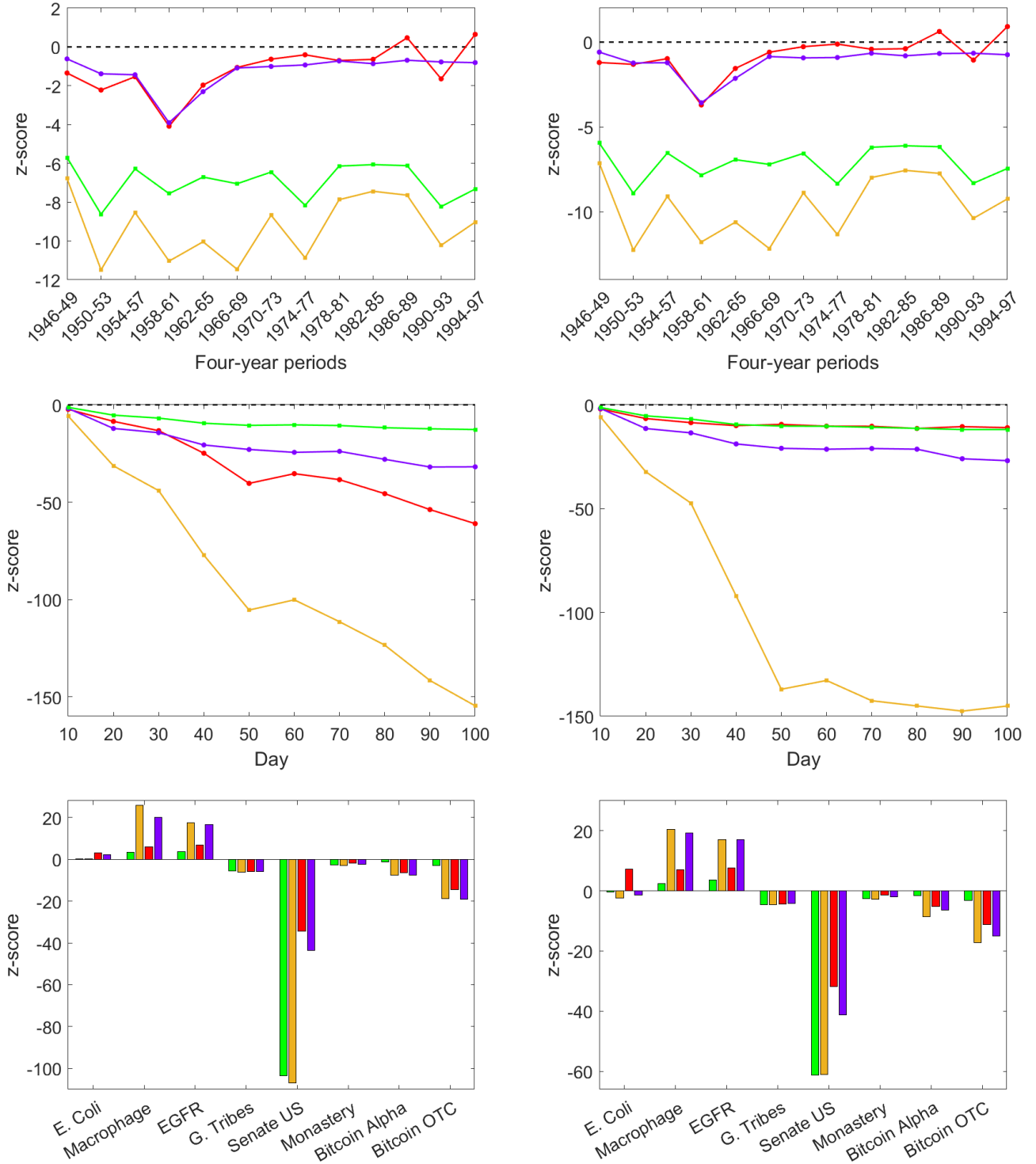


FIG. 6: Analysis of the z -scores of the SFI defined in Eq. 8 (left panel) and the WFI defined in Eq. 9 (right panel). Top panels refer to the 13 snapshots of 4 years each of the CoW dataset (covering the period 1946-1997). Middle panels refer to the snapshots of the MMOG dataset. Bottom panels refer to our additional set of social and biological networks. z -scores are computed under the SRGM (green), the SRGM-FT (orange), the SCM (red) and the SCM-FT (purple). We see that, with respect to all null models, frustration is under-represented in all social network data and over-represented in all biological data.

served in terms of their support for WBT or SBT.

Motivated by the last observation, we now use the

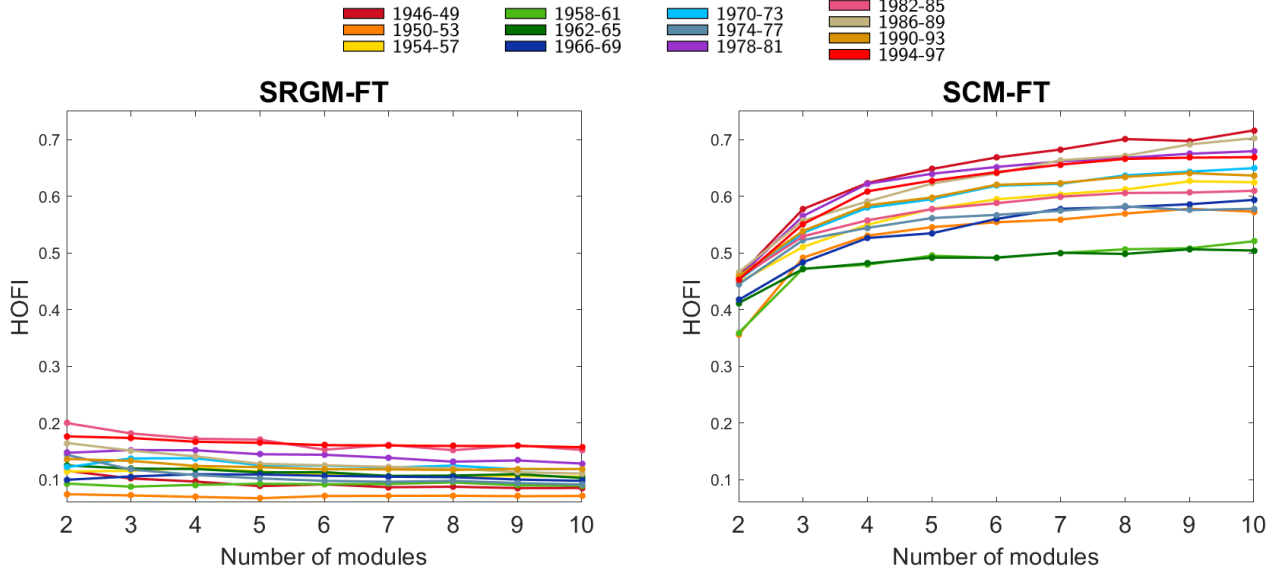


FIG. 7: Value of the HOFI on various optimal partitions of the 13 snapshots (of 4 years each) of the CoW dataset, each obtained by maximizing the modularity $Q = -L \cdot (\text{HOFI} - \langle \text{HOFI} \rangle)$ for a given number K of modules (communities), using as null models the SRGM-FT (left) and the SCM-FT (right). While the SRGM-FT reveals a rather flat profile of HOFI as a function of K , with the minimum obtained for a number of groups which is larger than two, the SCM-FT reveals that HOFI is always clearly minimized for a number of groups $K = 2$. Taken together, these results extend our findings at the mesoscale level.

null models with fixed topology to probe the patterns of structural (im)balance at a larger, mesoscopic level, i.e. as portrayed by the community structure deriving from optimally partitioning the nodes into communities with positive internal links and negative external ones. As anticipated, SBT predicts that the overall level of intra-community frustration, as measured by the HOFI defined in Eq. 10, should be observed after optimally partitioning the nodes into two communities, dominated by positive signs internally and negative signs across. By contrast, WBT allows for potentially any number of communities, because it bases the idea of balance precisely at the level of communities, so that all-negative triangles (and in principle all-negative cycles of any length) can be explained by placing the constituent nodes across distinct communities. To extract information about the signed community structure from our data, given a null model $\langle a_{ij} \rangle$ for the signed adjacency matrix entry a_{ij} , we consider the definition of signed modularity [46]

$$\begin{aligned}
 Q &= \sum_{i=1}^N \sum_{j<i} [a_{ij}^* - \langle a_{ij} \rangle] \delta_{c_i c_j} \\
 &= \sum_{i=1}^N \sum_{j<i} [(a_{ij}^+)^* - (a_{ij}^-)^* - (p_{ij}^+ - p_{ij}^-)] \delta_{c_i c_j} \\
 &= L_{\bullet}^+ - L_{\bullet}^- - \langle L_{\bullet}^+ - L_{\bullet}^- \rangle \\
 &= -[(L_{\circ}^+ + L_{\circ}^-) - \langle L_{\circ}^+ + L_{\circ}^- \rangle]
 \end{aligned} \tag{35}$$

(note that $L_{\bullet}^+ = L^+ - L_{\circ}^+$ and the total number of positive links is preserved under any null model considered here) and look for the partition that maximizes Q . Notably, for null models with fixed topology, a stronger result holds true, i.e. $Q = -L \cdot (\text{HOFI} - \langle \text{HOFI} \rangle)$ so that, since $L > 0$, maximizing Q becomes equivalent to minimizing the difference between HOFI and its expected value (see Appendix E). Notably, the minimization of HOFI is another popular approach to finding the optimal partition [47] which, however, neglects the information embodied in a null model. Here, we consider a varying number $K = 2, \dots, 10$ of communities and, for each value of K , look for the partition maximizing Q , using as null model both the SRGM-FT and the SCM-FT. We then compute the value of HOFI as a function of K , as plotted in Fig. 7 for the CoW dataset. We find that the trends produced under the SRGM-FT are quite flat, and in no case the minimum of HOFI is achieved by $K = 2$. This result is in line with WBT, under whose assumptions there is no specific characteristic number of communities that would characterize real networks. By contrast, the SCM-FT produces clearly increasing trends, all starting from a minimum of HOFI at $K = 2$. This result strongly supports SBT, according to which structural balance can be achieved by placing negative links between two communities, and positive links inside them. Taken together, these results extend our finding that WBT (SBT) is supported by homogeneous (heterogeneous) null models.

CONCLUSIONS

Motivated by the widespread observation that actors in real social networks are characterized by a strong heterogeneity (typically signalled by broad distributions of node-specific topological properties), we have introduced a class of null models for signed networks characterized by either global or local constraints and with either fixed or varying topology. Our formalism provides the equivalent of various important ERGs to the domain of signed graphs. We have used our null models to address the problem of structural balance in real social networks. Our results show that the nature (weak or strong) and statistical strength of evidence of structural balance strongly depends on the null model adopted. In particular, we have shown that the occurrences of signed triangles favour WBT when a homogeneous, global null model is considered. By contrast, SBT is favoured by heterogeneous models with local constraints. Generally speaking, adopting fixed-topology benchmarks seems to enhance the detection of frustration with the corresponding, homogeneous (heterogeneous) variant favouring WBT (SBT). As a possible behavioural explanation, one might conjecture that agents that cannot choose with whom to interact, but only ‘how’, adopt a seemingly ‘intolerant’ behaviour, strongly avoiding to engage in frustrated relationships; on the other hand, agents that are free to choose their neighbours seem to be more ‘tolerant’, as they establish a significantly large number of patterns composed by entirely positive edges while accepting a potential, ‘residual’ level of frustration. The same results have been extended to the mesoscale structural level, by finding that the optimal number of communities minimizing the overall level of frustration is $K = 2$ with respect to a heterogeneous null model (strongly supporting SBT), while there is no characteristic optimal number with respect to a homogeneous null model (in line with WBT). Importantly, we have considered a set of biological networks as a benchmark of real-world systems for which structural balance theory is not expected to apply. We have found a strong degree of frustration in biological systems, indicating that structural balance (in either strong or weak form) indeed characterizes social networks.

[1] T. Antal, P. L. Krapivsky, and S. Redner, Social balance on networks: The dynamics of friendship and enmity, *Physica D: Nonlinear Phenomena* **224**, 130 (2006).
 [2] J. Leskovec, D. Huttenlocher, and J. Kleinberg, Signed networks in social media, in *Proceedings of the SIGCHI Conference on Human Factors in Computing Systems* (2010) pp. 1361–1370.
 [3] T. Zaslavsky, A Mathematical Bibliography of Signed and Gain Graphs and Allied Areas, *The Electronic Journal of Combinatorics*, **DS8** (2012).

[4] J. Tang, Y. Chang, C. Aggarwal, and H. Liu, A Survey of Signed Network Mining in Social Media, *ACM Computing Surveys (CSUR)* **49**, 1 (2016).
 [5] F. Heider, Attitudes and Cognitive Organization, *The Journal of Psychology* **21**, 107 (1946).
 [6] D. Cartwright and F. Harary, Structural balance: a generalization of Heider’s theory., *Psychological Review* **63**, 277 (1956).
 [7] F. Harary, M.-H. Lim, and D. C. Wunsch, Signed graphs for portfolio analysis in risk management, *IMA Journal of Management Mathematics* **13**, 201 (2002).
 [8] L. Ou-Yang, D.-Q. Dai, and X.-F. Zhang, Detecting Protein Complexes from Signed Protein-Protein Interaction Networks, *IEEE/ACM Transactions on Computational Biology and Bioinformatics* **12**, 1333 (2015).
 [9] F. Iorio, M. Bernardo-Faura, A. Gobbi, T. Cokelaer, G. Jurman, and J. Saez-Rodriguez, Efficient randomization of biological networks while preserving functional characterization of individual nodes, *BMC Bioinformatics* **17**, 1 (2016).
 [10] H. Saiz, J. Gómez-Gardeñes, P. Nuche, A. Girón, Y. Pueyo, and C. L. Alados, Evidence of structural balance in spatial ecological networks, *Ecography* **40**, 733 (2017).
 [11] J. A. Davis, Clustering and Structural Balance in Graphs, *Human Relations* **20**, 181 (1967).
 [12] J. Akiyama, D. Avis, V. Chvátal, and H. Era, Balancing signed graphs, *Discrete Applied Mathematics* **3**, 227 (1981).
 [13] F. Harary, On the measurement of structural balance, *Behavioral Science* **4**, 316 (1959).
 [14] E. Estrada and M. Benzi, Walk-based measure of balance in signed networks: Detecting lack of balance in social networks, *Physical Review E* **90**, 042802 (2014).
 [15] R. Singh and B. Adhikari, Measuring the balance of signed networks and its application to sign prediction, *Journal of Statistical Mechanics: Theory and Experiment* **2017**, 063302 (2017).
 [16] E. Estrada, Rethinking structural balance in signed social networks, *Discrete Applied Mathematics* **268**, 70 (2019).
 [17] A. Kirkley, G. T. Cantwell, and M. E. Newman, Balance in signed networks, *Physical Review E* **99**, 012320 (2019).
 [18] D. Easley, J. Kleinberg, *et al.*, Networks, crowds, and markets, *Cambridge Books* (2012).
 [19] S. Aref, L. Dinh, R. Rezapour, and J. Diesner, Multilevel structural evaluation of signed directed social networks based on balance theory, *Scientific Reports* **10**, 1 (2020).
 [20] J. Kunegis, S. Schmidt, A. Lommatzsch, J. Lerner, E. W. De Luca, and S. Albayrak, Spectral Analysis of Signed Graphs for Clustering, Prediction and Visualization, in *Proceedings of the 2010 SIAM International Conference on Data Mining* (SIAM, 2010) pp. 559–570.
 [21] E. Terzi and M. Winkler, A Spectral Algorithm for Computing Social Balance, in *International Workshop on Algorithms and Models for the Web-Graph* (Springer, 2011) pp. 1–13.
 [22] P. Anchuri and M. Magdon-Ismael, Communities and Balance in Signed Networks: A Spectral Approach, in *2012 IEEE/ACM International Conference on Advances in Social Networks Analysis and Mining* (IEEE, 2012) pp. 235–242.
 [23] A. M. Belaza, K. Hoefman, J. Ryckebusch, A. Bramson, M. van den Heuvel, and K. Schoors, Statistical physics of balance theory, *PLoS One* **12**, e0183696 (2017).

- [24] T. Zaslavsky, Balanced decompositions of a signed graph, *Journal of Combinatorial Theory, Series B* **43**, 1 (1987).
- [25] S. Aref and M. C. Wilson, Balance and Frustration in Signed Networks, *Journal of Complex Networks* **7**, 163 (2019).
- [26] S. Aref, A. J. Mason, and M. C. Wilson, A modeling and computational study of the frustration index in signed networks, *Networks* **75**, 95 (2020).
- [27] V. Traag, P. Doreian, and A. Mrvar, Partitioning Signed Networks, *Advances in Network Clustering and Block-modeling*, 225 (2019).
- [28] R. P. Abelson and M. J. Rosenberg, Symbolic psychology: A model of attitudinal cognition, *Behavioral Science* **3**, 1 (1958).
- [29] G. Facchetti, G. Iacono, and C. Altafini, Computing global structural balance in large-scale signed social networks, *Proceedings of the National Academy of Sciences* **108**, 20953 (2011).
- [30] T. Derr, C. Aggarwal, and J. Tang, Signed Network Modeling Based on Structural Balance Theory, in *Proceedings of the 27th ACM International Conference on Information and Knowledge Management* (2018) pp. 557–566.
- [31] G. Huitsing, M. A. Van Duijn, T. A. Snijders, P. Wang, M. Sainio, C. Salmivalli, and R. Veenstra, Univariate and multivariate models of positive and negative networks: Liking, disliking, and bully–victim relationships, *Social Networks* **34**, 645 (2012).
- [32] J. Lerner, Structural balance in signed networks: Separating the probability to interact from the tendency to fight, *Social Networks* **45**, 66 (2016).
- [33] C. Becatti, G. Caldarelli, and F. Saracco, Entropy-based randomization of rating networks, *Physical Review E* **99**, 022306 (2019).
- [34] C. Fritz, M. Mehrl, P. W. Thurner, *et al.*, Exponential Random Graph Models for Dynamic Signed Networks: An Application to International Relations, *arXiv preprint arXiv:2205.13411* (2022).
- [35] E. Marchese, G. Caldarelli, and T. Squartini, Detecting mesoscale structures by surprise, *Communications Physics* **5**, 1 (2022).
- [36] J. Park and M. E. J. Newman, Statistical mechanics of networks, *Phys. Rev. E* **70**, 66117 (2004).
- [37] T. Squartini and D. Garlaschelli, *Maximum-Entropy Networks. Pattern Detection, Network Reconstruction and Graph Combinatorics* (Springer International Publishing, 2017) p. 116.
- [38] A. El Maftouhi, Y. Manoussakis, and O. Megalakaki, Balance in Random Signed Graphs, *Internet Mathematics* **8**, 364 (2012).
- [39] D. Garlaschelli and M. I. Loffredo, Maximum likelihood: Extracting unbiased information from complex networks, *Physical Review E* **78**, 015101 (2008).
- [40] N. Vallarano, M. Bruno, E. Marchese, G. Trapani, F. Saracco, G. Cimini, M. Zanon, and T. Squartini, Fast and scalable likelihood maximization for Exponential Random Graph Models with local constraints, *Scientific Reports* **11**, 15227 (2021).
- [41] P. Doreian and A. Mrvar, Structural Balance and Signed International Relations, *Journal of Social Structure* **16**, 1 (2015).
- [42] M. Szell, R. Lambiotte, and S. Thurner, Multirelational organization of large-scale social networks in an online world, *Proceedings of the National Academy of Sciences* **107**, 13636 (2010).
- [43] Signed networks from sociology and political science, systems biology, international relations, finance, and computational chemistry (2018).
- [44] S. F. Sampson, *A novitiate in a period of change: An experimental and case study of social relationships* (Cornell University, 1968).
- [45] S. Kumar, F. Spezzano, V. Subrahmanian, and C. Faloutsos, Edge Weight Prediction in Weighted Signed Networks, in *2016 IEEE 16th International Conference on Data Mining (ICDM)* (IEEE, 2016) pp. 221–230.
- [46] S. Gómez, P. Jensen, and A. Arenas, Analysis of community structure in networks of correlated data, *Physical Review E* **80**, 016114 (2009).
- [47] P. Doreian and A. Mrvar, A partitioning approach to structural balance, *Social Networks* **18**, 149 (1996).

APPENDIX A. REPRESENTING BINARY, UNDIRECTED, SIGNED NETWORKS

The three functions $a_{ij}^- = [a_{ij} = -1]$, $a_{ij}^0 = [a_{ij} = 0]$ and $a_{ij}^+ = [a_{ij} = +1]$ have been defined via the Iverson's brackets notation. Iverson's brackets work in a way that is reminiscent of the Heaviside step function, i.e. $\Theta[x] = [x > 0]$; in fact,

$$a_{ij}^- = [a_{ij} = -1] = \begin{cases} 1, & \text{if } a_{ij} = -1 \\ 0, & \text{if } a_{ij} = 0, +1 \end{cases} \quad (36)$$

(i.e. $a_{ij}^- = 1$ if $a_{ij} < 0$ and zero otherwise),

$$a_{ij}^0 = [a_{ij} = 0] = \begin{cases} 1, & \text{if } a_{ij} = 0 \\ 0, & \text{if } a_{ij} = -1, +1 \end{cases} \quad (37)$$

(i.e. $a_{ij}^0 = 1$ if $a_{ij} = 0$ and zero otherwise),

$$a_{ij}^+ = [a_{ij} = +1] = \begin{cases} 1, & \text{if } a_{ij} = +1 \\ 0, & \text{if } a_{ij} = -1, 0 \end{cases} \quad (38)$$

(i.e. $a_{ij}^+ = 1$ if $a_{ij} > 0$ and zero otherwise). The matrices $\mathbf{A}^+ \equiv \{a_{ij}^+\}_{i,j=1}^N$ and $\mathbf{A}^- \equiv \{a_{ij}^-\}_{i,j=1}^N$, thus, remain naturally defined and induce the relationships $\mathbf{A} = \mathbf{A}^+ - \mathbf{A}^-$, i.e. $a_{ij} = a_{ij}^+ - a_{ij}^-$, $\forall i \neq j$ and $|\mathbf{A}| = \mathbf{A}^+ + \mathbf{A}^-$, i.e. $|a_{ij}| = a_{ij}^+ + a_{ij}^-$, $\forall i \neq j$.

APPENDIX B. COUNTING TRIANGLES ON BINARY, UNDIRECTED, SIGNED NETWORKS

A well-known result states that the abundance of node-specific, unsigned triangles reads

$$2T_i = \sum_{\substack{j=1 \\ (j \neq i)}}^N \sum_{\substack{k=1 \\ (k \neq i, j)}}^N a_{ij} a_{jk} a_{ki} = [\mathbf{A}\mathbf{A}\mathbf{A}]_{ii} = [\mathbf{A}]_{ii}^3 \quad \forall i; \quad (39)$$

let us, now, consider signed networks: the abundances of node-specific, signed triangles with an even number of negative links read

$$T_i^{(+++)} = \sum_{\substack{j=1 \\ (j \neq i)}}^N \sum_{\substack{k=1 \\ (k \neq i, j)}}^N \frac{a_{ij}^+ a_{jk}^+ a_{ki}^+}{2} = \frac{[\mathbf{A}^+ \mathbf{A}^+ \mathbf{A}^+]_{ii}}{2} = \frac{[\mathbf{A}^+]_{ii}^3}{2} \quad \forall i, \quad (40)$$

$$T_i^{(-+-)} = \sum_{\substack{j=1 \\ (j \neq i)}}^N \sum_{\substack{k=1 \\ (k \neq i, j)}}^N \frac{a_{ij}^- a_{jk}^+ a_{ki}^-}{2} = \frac{[\mathbf{A}^- \mathbf{A}^+ \mathbf{A}^-]_{ii}}{2} \quad \forall i, \quad (41)$$

$$T_i^{(+--)} = \sum_{\substack{j=1 \\ (j \neq i)}}^N \sum_{\substack{k=1 \\ (k \neq i, j)}}^N \frac{a_{ij}^+ a_{jk}^- a_{ki}^-}{2} = [\mathbf{A}^+ \mathbf{A}^- \mathbf{A}^-]_{ii} = [\mathbf{A}^+ (\mathbf{A}^-)^2]_{ii} \quad \forall i, \quad (42)$$

$$T_i^{(--+)} = \sum_{\substack{j=1 \\ (j \neq i)}}^N \sum_{\substack{k=1 \\ (k \neq i, j)}}^N \frac{a_{ij}^- a_{jk}^- a_{ki}^+}{2} = [\mathbf{A}^- \mathbf{A}^- \mathbf{A}^+]_{ii} = [(\mathbf{A}^-)^2 \mathbf{A}^+]_{ii} \quad \forall i \quad (43)$$

while the abundances of node-specific, signed triangles with an odd number of negative links read

$$T_i^{(---)} = \sum_{\substack{j=1 \\ (j \neq i)}}^N \sum_{\substack{k=1 \\ (k \neq i, j)}}^N \frac{a_{ij}^- a_{jk}^- a_{ki}^-}{2} = \frac{[\mathbf{A}^- \mathbf{A}^- \mathbf{A}^-]_{ii}}{2} = \frac{[\mathbf{A}^-]_{ii}^3}{2} \quad \forall i, \quad (44)$$

$$T_i^{(+++)} = \sum_{\substack{j=1 \\ (j \neq i)}}^N \sum_{\substack{k=1 \\ (k \neq i, j)}}^N \frac{a_{ij}^+ a_{jk}^+ a_{ki}^+}{2} = \frac{[\mathbf{A}^+ \mathbf{A}^+ \mathbf{A}^+]_{ii}}{2} \quad \forall i, \quad (45)$$

$$T_i^{(++)-} = \sum_{\substack{j=1 \\ (j \neq i)}}^N \sum_{\substack{k=1 \\ (k \neq i, j)}}^N a_{ij}^+ a_{jk}^+ a_{ki}^- = [\mathbf{A}^+ \mathbf{A}^+ \mathbf{A}^-]_{ii} = [(\mathbf{A}^+)^2 \mathbf{A}^-]_{ii} \quad \forall i, \quad (46)$$

$$T_i^{(-++)} = \sum_{\substack{j=1 \\ (j \neq i)}}^N \sum_{\substack{k=1 \\ (k \neq i, j)}}^N a_{ij}^- a_{jk}^+ a_{ki}^+ = [\mathbf{A}^- \mathbf{A}^+ \mathbf{A}^+]_{ii} = [\mathbf{A}^- (\mathbf{A}^+)^2]_{ii} \quad \forall i. \quad (47)$$

Let us, now, write the expressions for the total abundances of signed triangles with an even number of negative links:

$$T^{(+++)} = \frac{1}{3} \sum_{i=1}^N T_i^{(+++)} = \frac{1}{6} \sum_{i=1}^N [\mathbf{A}^+ \mathbf{A}^+ \mathbf{A}^+]_{ii} = \frac{\text{Tr}[\mathbf{A}^+ \mathbf{A}^+ \mathbf{A}^+]}{6} = \frac{\text{Tr}[(\mathbf{A}^+)^3]}{6}, \quad (48)$$

$$T^{(---)} = \frac{1}{2} \sum_{i=1}^N T_i^{(---)} = \frac{1}{2} \sum_{i=1}^N [\mathbf{A}^- \mathbf{A}^- \mathbf{A}^-]_{ii} = \frac{\text{Tr}[\mathbf{A}^- \mathbf{A}^- \mathbf{A}^-]}{2}, \quad (49)$$

$$T^{(+-+)} = \frac{1}{2} \sum_{i=1}^N T_i^{(+-+)} = \frac{1}{2} \sum_{i=1}^N [\mathbf{A}^+ \mathbf{A}^- \mathbf{A}^-]_{ii} = \frac{\text{Tr}[\mathbf{A}^+ \mathbf{A}^- \mathbf{A}^-]}{2} = \frac{\text{Tr}[\mathbf{A}^+ (\mathbf{A}^-)^2]}{2}, \quad (50)$$

$$T^{(-+-)} = \frac{1}{2} \sum_{i=1}^N T_i^{(-+-)} = \frac{1}{2} \sum_{i=1}^N [\mathbf{A}^- \mathbf{A}^+ \mathbf{A}^+]_{ii} = \frac{\text{Tr}[\mathbf{A}^- \mathbf{A}^+ \mathbf{A}^+]}{2} = \frac{\text{Tr}[(\mathbf{A}^-)^2 \mathbf{A}^+]}{2}; \quad (51)$$

analogously, for the abundances of triangles with an odd number of negative links, reading

$$T^{(---)} = \frac{1}{3} \sum_{i=1}^N T_i^{(---)} = \frac{1}{6} \sum_{i=1}^N [\mathbf{A}^- \mathbf{A}^- \mathbf{A}^-]_{ii} = \frac{\text{Tr}[\mathbf{A}^- \mathbf{A}^- \mathbf{A}^-]}{6} = \frac{\text{Tr}[(\mathbf{A}^-)^3]}{6}, \quad (52)$$

$$T^{(---)} = \frac{1}{2} \sum_{i=1}^N T_i^{(---)} = \frac{1}{2} \sum_{i=1}^N [\mathbf{A}^+ \mathbf{A}^- \mathbf{A}^+]_{ii} = \frac{\text{Tr}[\mathbf{A}^+ \mathbf{A}^- \mathbf{A}^+]}{2}, \quad (53)$$

$$T^{(---)} = \frac{1}{2} \sum_{i=1}^N T_i^{(---)} = \frac{1}{2} \sum_{i=1}^N [\mathbf{A}^+ \mathbf{A}^+ \mathbf{A}^-]_{ii} = \frac{\text{Tr}[\mathbf{A}^+ \mathbf{A}^+ \mathbf{A}^-]}{2} = \frac{\text{Tr}[(\mathbf{A}^+)^2 \mathbf{A}^-]}{2}, \quad (54)$$

$$T^{(---)} = \frac{1}{2} \sum_{i=1}^N T_i^{(---)} = \frac{1}{2} \sum_{i=1}^N [\mathbf{A}^- \mathbf{A}^+ \mathbf{A}^+]_{ii} = \frac{\text{Tr}[\mathbf{A}^- \mathbf{A}^+ \mathbf{A}^+]}{2} = \frac{\text{Tr}[\mathbf{A}^- (\mathbf{A}^+)^2]}{2} \quad (55)$$

(where each numeric factor avoids the corresponding pattern to be overcounted).

Since the trace of a matrix is invariant under a cyclic permutation of the members of its argument, the following result holds true

$$\frac{\text{Tr}[\mathbf{A}^+ \mathbf{A}^- \mathbf{A}^-]}{2} = \frac{\text{Tr}[\mathbf{A}^- \mathbf{A}^+ \mathbf{A}^-]}{2} = \frac{\text{Tr}[\mathbf{A}^- \mathbf{A}^- \mathbf{A}^+]}{2} \quad (56)$$

further implying that $T^{(+-+)} = T^{(-+-)} = T^{(---)}$. As a consequence, the number of balanced patterns according to either variant of the BT can be defined in several, equivalent ways, i.e. $\#_{\Delta}^{sb} = T^{(+++)} + T^{(+-+)} = T^{(+++)} + T^{(-+-)} =$

$T^{(+++)} + T^{(---)}$; analogously, $\#_{\Delta}^{wb} = T^{(+++)} + T^{(+--)} + T^{(---)} = T^{(+++)} + T^{(+--)} + T^{(---)} = T^{(+++)} + T^{(+--)} + T^{(---)}$.

APPENDIX C. PROBABILISTIC MODELS FOR BINARY, UNDIRECTED, SIGNED NETWORKS

The generalization of the ERG formalism for the analysis of binary, undirected, signed graphs rests upon the constrained maximization of Shannon entropy, i.e.

$$\mathcal{L} = S[P] - \sum_{i=0}^M \theta_i [P(\mathbf{A})C_i(\mathbf{A}) - \langle C_i \rangle] \quad (57)$$

where $S = -\sum_{\mathbf{A} \in \mathbb{A}} P(\mathbf{A}) \ln P(\mathbf{A})$, $C_0 \equiv \langle C_0 \rangle \equiv 1$ sums up the normalization condition and the remaining $M - 1$ constraints represent proper, topological properties. Such an optimization procedure defines the expression

$$P(\mathbf{A}) = \frac{e^{-H(\mathbf{A})}}{Z} = \frac{e^{-H(\mathbf{A})}}{\sum_{\mathbf{A} \in \mathbb{A}} e^{-H(\mathbf{A})}} = \frac{e^{-\sum_{i=1}^M \theta_i C_i(\mathbf{A})}}{\sum_{\mathbf{A} \in \mathbb{A}} e^{-\sum_{i=1}^M \theta_i C_i(\mathbf{A})}} \quad (58)$$

that can be made explicit only after a specific set of constraints has been chosen.

Signed Random Graph Model

The first set of constraints we consider is represented by the properties $L^+(\mathbf{A})$ and $L^-(\mathbf{A})$. The Hamiltonian describing such a problem reads

$$H(\mathbf{A}) = \alpha L^+(\mathbf{A}) + \beta L^-(\mathbf{A}); \quad (59)$$

as a consequence, the partition function reads

$$\begin{aligned} Z &= \sum_{\mathbf{A} \in \mathbb{A}} e^{-H(\mathbf{A})} = \sum_{\mathbf{A} \in \mathbb{A}} e^{-\alpha L^+(\mathbf{A}) - \beta L^-(\mathbf{A})} = \sum_{\mathbf{A} \in \mathbb{A}} e^{-\sum_{i=1}^N \sum_{j(>i)=1}^N (\alpha a_{ij}^+ + \beta a_{ij}^-)} = \sum_{\mathbf{A} \in \mathbb{A}} \prod_{i=1}^N \prod_{\substack{j=1 \\ (j>i)}}^N e^{-\alpha a_{ij}^+ - \beta a_{ij}^-} \\ &= \prod_{i=1}^N \prod_{\substack{j=1 \\ (j>i)}}^N \sum_{a_{ij} = -1, 0, 1} e^{-\alpha a_{ij}^+ - \beta a_{ij}^-} = \prod_{i=1}^N \prod_{\substack{j=1 \\ (j>i)}}^N (1 + e^{-\alpha} + e^{-\beta}) = (1 + e^{-\alpha} + e^{-\beta})^{\binom{N}{2}} \end{aligned} \quad (60)$$

and induces the expression

$$P_{\text{SRGM}}(\mathbf{A}) = \frac{e^{-\alpha L^+(\mathbf{A}) - \beta L^-(\mathbf{A})}}{(1 + e^{-\alpha} + e^{-\beta})^{\binom{N}{2}}} \equiv \frac{x^{L^+(\mathbf{A})} y^{L^-(\mathbf{A})}}{(1 + x + y)^{\binom{N}{2}}} \equiv (p^-)^{L^-} (p^0)^{L^0} (p^+)^{L^+} \quad (61)$$

having posed $p^- \equiv \frac{e^{-\beta}}{1 + e^{-\alpha} + e^{-\beta}} \equiv \frac{y}{1 + x + y}$, $p^0 \equiv \frac{1}{1 + e^{-\alpha} + e^{-\beta}} \equiv \frac{1}{1 + x + y}$ and $p^+ \equiv \frac{e^{-\alpha}}{1 + e^{-\alpha} + e^{-\beta}} \equiv \frac{x}{1 + x + y}$, where p^+ is the probability that any two nodes are linked by a positive edge, p^- is the probability that any two nodes are linked by a negative edge and p^0 is the probability that any two nodes are no linked at all. Hence, according to the SRGM, each entry of a signed network is a random variable following a generalized Bernoulli distribution, i.e. obeying the finite scheme

$$a_{ij} \sim \begin{pmatrix} -1 & 0 & +1 \\ p^- & p^0 & p^+ \end{pmatrix} \quad \forall i < j; \quad (62)$$

notice that while the expected value of the random variable a_{ij} reads $\langle a_{ij} \rangle = p^+ - p^-$, its variance reads $\text{Var}[a_{ij}] = p^-[1 + (p^+ - p^-)] + p^+[1 - (p^+ - p^-)]$. As a consequence, any network belonging to \mathbf{A} is a collection of i.i.d. random variables and obeys the finite scheme

$$\mathbf{A} \sim \bigotimes \begin{pmatrix} -1 & 0 & +1 \\ p^- & p^0 & p^+ \end{pmatrix} \quad (63)$$

i.e. the directed product of the $\binom{N}{2}$ finite schemes above.

The probability, under the SRGM, that a graph has exactly L^+ positive links and L^- negative links reads

$$P(L^-, L^+) = \binom{\binom{N}{2}}{L^-, L^0, L^+} (p^-)^{L^-} (p^0)^{L^0} (p^+)^{L^+}; \quad (64)$$

in other words, it is a multinomial distribution, i.e. a generalization of the binomial distribution in case there are more than two, possible outcomes for each trial. The combinatorial factor

$$\binom{\binom{N}{2}}{L^-, L^0, L^+} = \frac{\binom{N}{2}!}{L^-! L^0! L^+!} \quad (65)$$

with $L^0 = \binom{N}{2} - L = \binom{N}{2} - (L^- + L^+)$, is the (multinomial) coefficient counting the total number of ways L links (L^+ of which are positive and L^- of which are negative) can be placed among the node-pairs. Hence, (65) also represents the total number of graphs with a given number of signed links.

Naturally, it is possible to define the marginal random variables $a_{ij}^+ \sim \text{Ber}(p^+)$ and $a_{ij}^- \sim \text{Ber}(p^-)$ which, in turn, induce the marginal probability distributions $P(L^-) = \text{Bin}\left(\binom{N}{2}, p^-\right)$, $P(L^0) = \text{Bin}\left(\binom{N}{2}, p^0\right)$ and $P(L^+) = \text{Bin}\left(\binom{N}{2}, p^+\right)$; from the latter ones, it follows that the total number of expected, positive links reads $\langle L^+ \rangle = \binom{N}{2} p^+$ while the total number of expected, negative links reads $\langle L^- \rangle = \binom{N}{2} p^-$. Obviously, $\langle L \rangle = \langle L^+ \rangle + \langle L^- \rangle = \binom{N}{2} (p^- + p^+) \equiv \binom{N}{2} p$. In other words, it is possible to define a ‘traditional’ Random Graph Model whose parameter is $p \equiv p(a_{ij} = -1) + p(a_{ij} = +1) = p^- + p^+$.

Let us, now, move to describe the behaviour of the degree. The probability, under the SRGM, that a node has exactly k^+ positive links and k^- negative links reads

$$P(k^-, k^+) = \binom{N-1}{k^-, k^0, k^+} (p^-)^{k^-} (p^0)^{k^0} (p^+)^{k^+}; \quad (66)$$

again, it obeys a multinomial distribution. The combinatorial factor

$$\binom{N-1}{k^-, k^0, k^+} = \frac{(N-1)!}{k^-! k^0! k^+!} \quad (67)$$

with $k^0 = (N-1) - k = (N-1) - (k^+ + k^-)$, is the (multinomial) coefficient counting the total number of ways k links (k^+ of which are positive and k^- of which are negative) can be placed among the $N-1$ node-pairs each node individuates. The marginal random variables $a_{ij}^+ \sim \text{Ber}(p^+)$ and $a_{ij}^- \sim \text{Ber}(p^-)$ also induce the marginal probability distributions $P(k^-) = \text{Bin}(N-1, p^-)$, $P(k^0) = \text{Bin}(N-1, p^0)$ and $P(k^+) = \text{Bin}(N-1, p^+)$; from the latter ones, it follows that the expected, positive degree reads $\langle k^+ \rangle = (N-1)p^+$ while the expected, negative degree reads $\langle k^- \rangle = (N-1)p^-$. Obviously, $\langle k \rangle = \langle k^+ \rangle + \langle k^- \rangle = (N-1)(p^- + p^+) \equiv (N-1)p$.

In order to determine the parameters that define the SRGM, let us maximize the likelihood function

$$\mathcal{L}_{\text{SRGM}}(x, y) \equiv \ln P_{\text{SRGM}}(\mathbf{A}^* | x, y) = L^+(\mathbf{A}^*) \ln(x) + L^-(\mathbf{A}^*) \ln(y) - \binom{N}{2} \ln(1 + x + y) \quad (68)$$

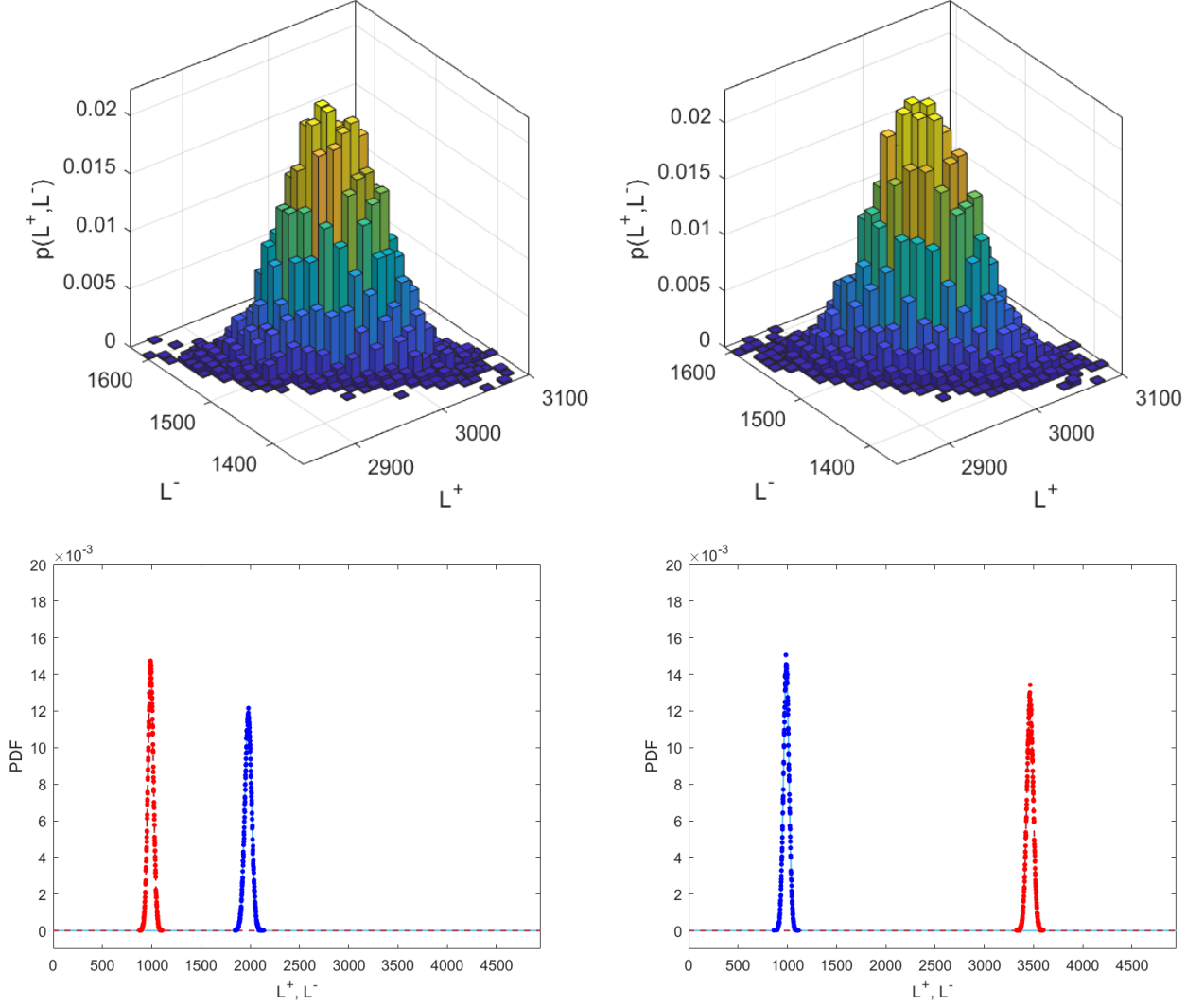


FIG. 8: Top panels: empirical, joint distribution of L^+ and L^- over an ensemble of 10.000 configurations induced by the SRGM whose parameters have been tuned to $N = 100$, $p^- = 0.2$, $p^0 = 0.3$ and $p^+ = 0.5$ (left) and multinomial distribution $\text{Multi}\left(\binom{N}{2}, \{p^-, p^0, p^+\}\right)$ (right): the two have been sided for a visual comparison. Bottom panels: distributions of L^+ (blue dots) and L^- (red dots) over an ensemble of 100.000 configurations induced by the SRGM whose parameters have been tuned to $N = 100$, $p^+ = 0.4$, $p^- = 0.2$ (left panel) and $N = 100$, $p^+ = 0.2$, $p^- = 0.7$ (right panel). The red, dashed lines represent the binomial distributions $\text{Bin}\left(\binom{N}{2}, p^-\right)$ while the blue, solid lines represent the binomial distributions $\text{Bin}\left(\binom{N}{2}, p^+\right)$.

with respect to x and y . Upon doing so, we obtain the pair of equations

$$\frac{\partial \mathcal{L}_{\text{SRGM}}(x, y)}{\partial x} = \frac{L^+(\mathbf{A}^*)}{x} - \binom{N}{2} \frac{1}{1+x+y}, \quad \frac{\partial \mathcal{L}_{\text{SRGM}}(x, y)}{\partial y} = \frac{L^-(\mathbf{A}^*)}{y} - \binom{N}{2} \frac{1}{1+x+y}; \quad (69)$$

equating them to zero leads us to find $L^+(\mathbf{A}^*) = \binom{N}{2} \frac{x}{1+x+y} = \binom{N}{2} p^+ = \langle L^+ \rangle$ and $L^-(\mathbf{A}^*) = \binom{N}{2} \frac{y}{1+x+y} = \binom{N}{2} p^- = \langle L^- \rangle$, i.e.

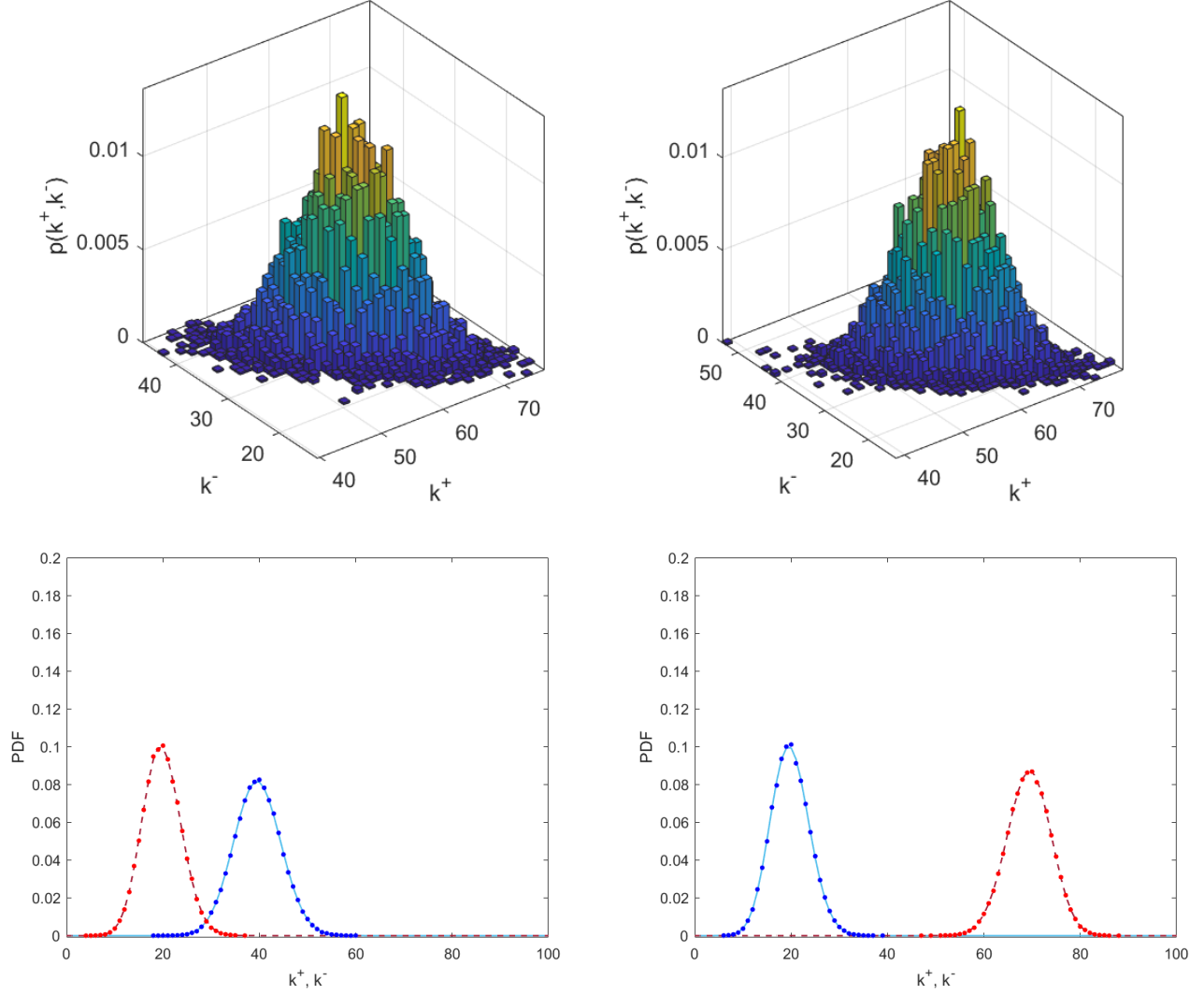


FIG. 9: Top panels: empirical, joint distribution of k^+ and k^- over an ensemble of 10.000 configurations induced by the SRGM whose parameters have been tuned to $N = 100$, $p^- = 0.3$, $p^0 = 0.1$ and $p^+ = 0.6$ (left) and multinomial distribution $\text{Multi}(N - 1, \{p^-, p^0, p^+\})$ (right): the two have been sided for a visual comparison. Bottom panels: distributions of k^+ (blue dots) and k^- (red dots), for an arbitrarily chosen node, over an ensemble of 100.000 configurations induced by the SRGM whose parameters have been tuned to $N = 100$, $p^+ = 0.4$, $p^- = 0.2$ (left panel) and $N = 100$, $p^+ = 0.2$, $p^- = 0.7$ (right panel). The red, dashed lines represent the binomial distributions $\text{Bin}(N - 1, p^-)$ while the blue, solid lines represent the binomial distributions $\text{Bin}(N - 1, p^+)$.

$$p^+ = \frac{2L^+(\mathbf{A}^*)}{N(N-1)}, \quad p^- = \frac{2L^-(\mathbf{A}^*)}{N(N-1)}. \quad (70)$$

Naturally, $p^0 \equiv 1 - p^- - p^+$.

Signed Random Graph Model with fixed topology

Let us, again, consider the properties $L^+(\mathbf{A})$ and $L^-(\mathbf{A})$, to be satisfied by keeping a network topology fixed. In what follows, we will indicate the adopted topology as the one induced by the matrix \mathbf{A}^* . The Hamiltonian describing such a problem still reads

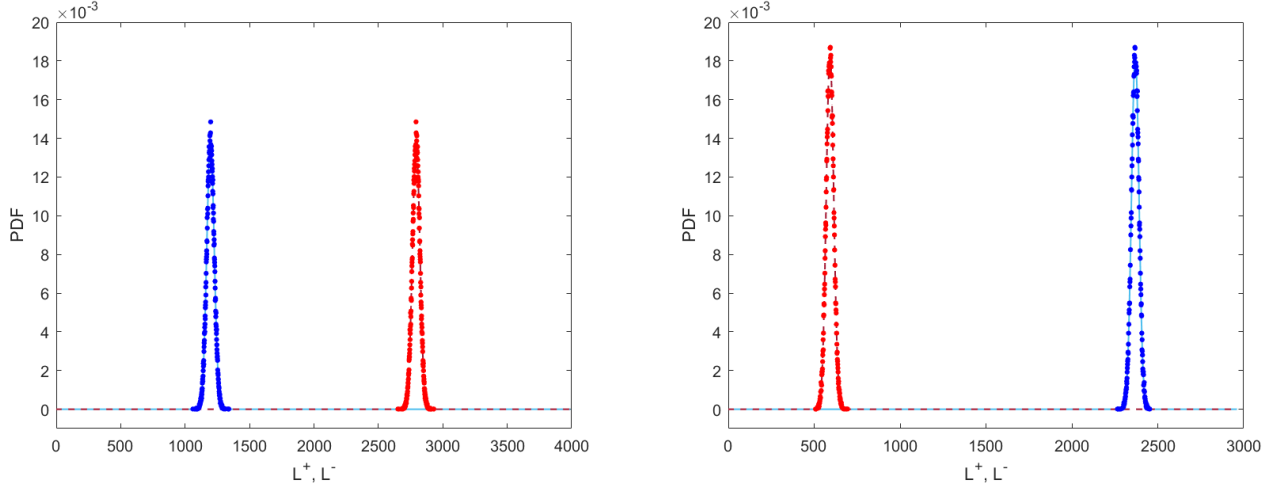


FIG. 10: Distributions of L^+ (blue dots) and L^- (red dots) over an ensemble of 100.000 configurations induced by the SRGM-FT whose parameters have been tuned to $N = 100$, $p^+ = 0.3$, $p^- = 0.7$ (left panel) and $N = 100$, $p^+ = 0.8$, $p^- = 0.2$ (right panel). The fixed topologies have been chosen by sampling a ‘traditional’ Random Graph Model with $p = 0.8$ (left panel) and $p = 0.6$ (right panel). The red, dashed lines represent the binomial distributions $\text{Bin}(L, p^-)$ while the blue, solid lines represent the binomial distributions $\text{Bin}(L, p^+)$.

$$H(\mathbf{A}) = \alpha L^+(\mathbf{A}) + \beta L^-(\mathbf{A}) \quad (71)$$

but induces a partition function reading

$$\begin{aligned} Z &= \sum_{\substack{\mathbf{A} \in \mathbb{A} \\ (|\mathbf{A}|=|\mathbf{A}^*)}} e^{-H(\mathbf{A})} = \sum_{\substack{\mathbf{A} \in \mathbb{A} \\ (|\mathbf{A}|=|\mathbf{A}^*)}} e^{-\alpha L^+(\mathbf{A}) - \beta L^-(\mathbf{A})} = \sum_{\substack{\mathbf{A} \in \mathbb{A} \\ (|\mathbf{A}|=|\mathbf{A}^*)}} e^{-\sum_{i=1}^N \sum_{j(>i)=1}^N (\alpha a_{ij}^+ + \beta a_{ij}^-)} = \sum_{\substack{\mathbf{A} \in \mathbb{A} \\ (|\mathbf{A}|=|\mathbf{A}^*)}} \prod_{i=1}^N \prod_{\substack{j=1 \\ (j>i)}}^N e^{-\alpha a_{ij}^+ - \beta a_{ij}^-} \\ &= \prod_{i=1}^N \prod_{\substack{j=1 \\ (j>i)}}^N \left(\sum_{a_{ij} = -1, 1} e^{-\alpha a_{ij}^+ - \beta a_{ij}^-} \right)^{|a_{ij}^*|} = \prod_{i=1}^N \prod_{\substack{j=1 \\ (j>i)}}^N (e^{-\alpha} + e^{-\beta})^{|a_{ij}^*|} = (e^{-\alpha} + e^{-\beta})^L; \end{aligned} \quad (72)$$

in other words, the support of the distribution becomes the set of node pairs i, j , with $i < j$, such that $|a_{ij}^*| = 1$, inducing a set of admissible configurations whose cardinality amounts at 2^L . The expression above leads us to find

$$P_{\text{SRGM-FT}}(\mathbf{A}) = \frac{e^{-\alpha L^+(\mathbf{A}) - \beta L^-(\mathbf{A})}}{(e^{-\alpha} + e^{-\beta})^L} \equiv \frac{x^{L^+(\mathbf{A})} y^{L^-(\mathbf{A})}}{(x + y)^L} \equiv (p^-)^{L^-} (p^+)^{L^+} \quad (73)$$

having posed $p^- \equiv \frac{e^{-\beta}}{e^{-\alpha} + e^{-\beta}} \equiv \frac{y}{x+y}$ and $p^+ \equiv \frac{e^{-\alpha}}{e^{-\alpha} + e^{-\beta}} \equiv \frac{x}{x+y}$ where p^+ is the probability that any two, connected nodes are linked by a positive edge and p^- is the probability that any two, connected nodes are linked by a negative edge. Hence, according to the SRGM-FT, the generic entry of a signed network satisfying $|a_{ij}| = |a_{ij}^*| = 1$ is a random variable following a Bernoulli distribution, i.e. obeying the finite scheme

$$a_{ij} \sim \begin{pmatrix} -1 & +1 \\ p^- & p^+ \end{pmatrix} \quad \forall i < j \mid |a_{ij}^*| = 1. \quad (74)$$

The probability, under the SRGM-FT, that a graph has exactly L^+ positive links reads

$$P(L^+) = \binom{L}{L^+} (p^-)^{L^-} (p^+)^{L^+} = \binom{L}{L^+} (p^+)^{L^+} (1 - p^+)^{L - L^+} \quad (75)$$

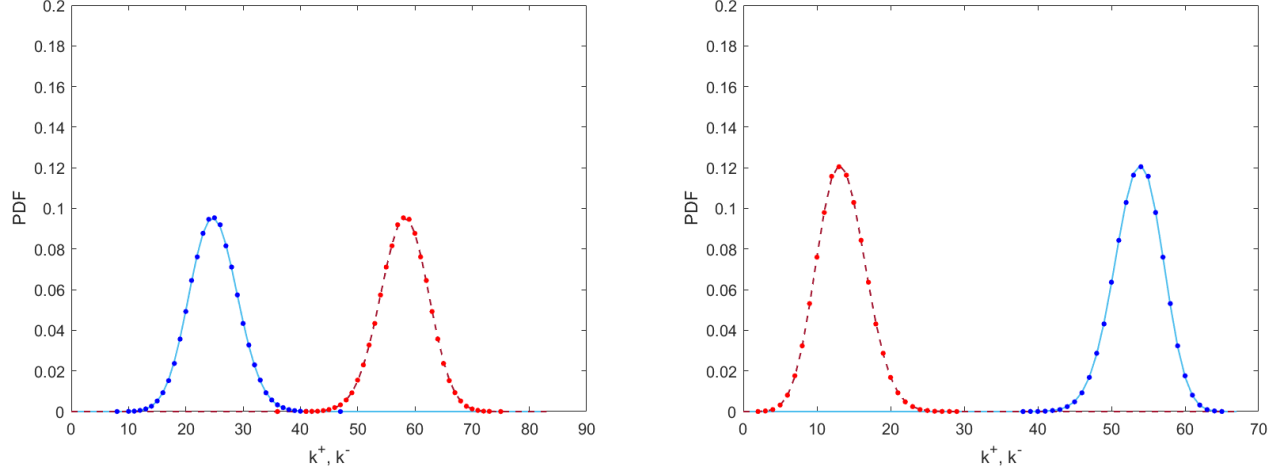


FIG. 11: Distributions of k^+ (blue dots) and k^- (red dots), for an arbitrarily chosen node, over an ensemble of 100.000 configurations induced by the SRGM-FT whose parameters have been tuned to $N = 100$, $p^+ = 0.3$, $p^- = 0.7$ (left panel) and $N = 100$, $p^+ = 0.8$, $p^- = 0.2$ (right panel). The fixed topologies have been chosen by sampling a ‘traditional’ Random Graph Model with $p = 0.8$ (left panel) and $p = 0.6$ (right panel). The red, dashed lines represent the binomial distributions $\text{Bin}(k, p^-)$ while the blue, solid lines represent the binomial distributions $\text{Bin}(k, p^+)$.

i.e. it is a binomial distribution, with L indicating the total number of unsigned links. As a consequence, the total number of expected, positive links reads $\langle L^+ \rangle = Lp^+$; analogously, $L^- \sim \text{Bin}(L, p^-)$. Similarly, the probability, under the SRGM-FT, that node i establishes exactly k_i^+ positive links reads

$$P(k_i^+) = \binom{k_i}{k_i^+} (p^-)^{k_i - k_i^+} (p^+)^{k_i^+} = \binom{k_i}{k_i^+} (p^+)^{k_i^+} (1 - p^-)^{k_i - k_i^+}; \quad (76)$$

again, it is a binomial distribution, with k_i indicating the unsigned degree of node i . As a consequence, the expected, positive degree of node i reads $\langle k_i^+ \rangle = k_i p^+$; analogously, $k_i^- \sim \text{Bin}(k_i, p^-)$.

In order to determine the parameters that define the SRGM-FT, let us maximize the likelihood function

$$\mathcal{L}_{\text{SRGM-FT}}(x, y) \equiv \ln P_{\text{SRGM-FT}}(\mathbf{A}^* | x, y) = L^+(\mathbf{A}^*) \ln(x) + L^-(\mathbf{A}^*) \ln(y) - L(\mathbf{A}^*) \ln(x + y) \quad (77)$$

with respect to x and y . Upon doing so, we obtain the pair of equations

$$\frac{\partial \mathcal{L}_{\text{SRGM-FT}}(x, y)}{\partial x} = \frac{L^+(\mathbf{A}^*)}{x} - \frac{L(\mathbf{A}^*)}{x + y}, \quad \frac{\partial \mathcal{L}_{\text{SRGM-FT}}(x, y)}{\partial y} = \frac{L^-(\mathbf{A}^*)}{y} - \frac{L(\mathbf{A}^*)}{x + y}; \quad (78)$$

equating them to zero leads us to find $L^+(\mathbf{A}^*) = L(\mathbf{A}^*) \frac{x}{x+y} = L(\mathbf{A}^*) p^+ = \langle L^+ \rangle$ and $L^-(\mathbf{A}^*) = L(\mathbf{A}^*) \frac{y}{x+y} = L(\mathbf{A}^*) p^- = \langle L^- \rangle$, i.e.

$$p^+ = \frac{L^+(\mathbf{A}^*)}{L(\mathbf{A}^*)}, \quad p^- = \frac{L^-(\mathbf{A}^*)}{L(\mathbf{A}^*)}. \quad (79)$$

Signed Random Graph Model: free VS fixed topology

In order to clarify the relationship between the SRGM and the SRGM-FT, let us write

$$\begin{aligned}
P_{\text{SRGM}}(\mathbf{A}) &= P_{\text{RGM}}(\mathbf{A}) \cdot \frac{P_{\text{SRGM}}(\mathbf{A})}{P_{\text{RGM}}(\mathbf{A})} \\
&= p^L (1-p)^{\binom{N}{2}-L} \cdot \frac{(p^-)^{L^-} (p^+)^{L^+} (1-p^- - p^+)^{\binom{N}{2}-L^- - L^+}}{p^L (1-p)^{\binom{N}{2}-L}} \\
&= p^L (1-p)^{\binom{N}{2}-L} \cdot \frac{(p^-)^{L^-} (p^+)^{L^+} (1-p^- - p^+)^{\binom{N}{2}-L^- - L^+}}{p^{L^-} p^{L^+} (1-p)^{\binom{N}{2}-L^- - L^+}} \\
&= p^L (1-p)^{\binom{N}{2}-L} \cdot \left(\frac{p^-}{p}\right)^{L^-} \left(\frac{p^+}{p}\right)^{L^+} \left(\frac{1-p^- - p^+}{1-p}\right)^{\binom{N}{2}-L^- - L^+}; \tag{80}
\end{aligned}$$

since the RGM induced by the SRGM satisfies the relationship $p \equiv p^- + p^+$, one has that

$$\begin{aligned}
P_{\text{SRGM}}(\mathbf{A}) &= p^L (1-p)^{\binom{N}{2}-L} \cdot \left(\frac{p^-}{p}\right)^{L^-} \left(\frac{p^+}{p}\right)^{L^+} \\
&= P_{\text{RGM}}(\mathbf{A}) \cdot P_{\text{SRGM-FT}}(\mathbf{A}) \tag{81}
\end{aligned}$$

the parameters defining the SRGM-FT being, now, p^-/p and p^+/p . Beside having an intuitive meaning, i.e.

$$\frac{p^-}{p} = \frac{p^-}{p^- + p^+} = \frac{P(\text{'link'} \cap \text{'link -'})}{P(\text{'link'})} = P(\text{'link -'} \mid \text{'link'}), \tag{82}$$

$$\frac{p^+}{p} = \frac{p^+}{p^- + p^+} = \frac{P(\text{'link'} \cap \text{'link +'})}{P(\text{'link'})} = P(\text{'link +' } \mid \text{'link'}) \tag{83}$$

these expressions are also consistent with the estimations of the parameters obtained via the likelihood maximization: in fact,

$$\frac{p^-}{p} = \frac{p^-}{p^- + p^+} = \frac{2L^-/N(N-1)}{2L^-/N(N-1) + 2L^+/N(N-1)} = \frac{2L^-/N(N-1)}{2L/N(N-1)} = \frac{L^-}{L}, \tag{84}$$

$$\frac{p^+}{p} = \frac{p^+}{p^- + p^+} = \frac{2L^+/N(N-1)}{2L^-/N(N-1) + 2L^+/N(N-1)} = \frac{2L^+/N(N-1)}{2L/N(N-1)} = \frac{L^+}{L}. \tag{85}$$

Signed Configuration Model

The second set of constraints we consider is represented by the properties $\{k_i^+(\mathbf{A})\}_{i=1}^N$ and $\{k_i^-(\mathbf{A})\}_{i=1}^N$. The Hamiltonian describing such a problem reads

$$H(\mathbf{A}) = \sum_{i=1}^N [\alpha_i k_i^+(\mathbf{A}) + \beta_i k_i^-(\mathbf{A})]; \tag{86}$$

as a consequence, the partition function reads

$$\begin{aligned}
Z &= \sum_{\mathbf{A} \in \mathbb{A}} e^{-H(\mathbf{A})} = \sum_{\mathbf{A} \in \mathbb{A}} e^{-\sum_{i=1}^N [\alpha_i k_i^+(\mathbf{A}) + \beta_i k_i^-(\mathbf{A})]} = \sum_{\mathbf{A} \in \mathbb{A}} e^{-\sum_{i=1}^N \sum_{j(>i)=1}^N [(\alpha_i + \alpha_j) a_{ij}^+ + (\beta_i + \beta_j) a_{ij}^-]} \\
&= \sum_{\mathbf{A} \in \mathbb{A}} \prod_{i=1}^N \prod_{\substack{j=1 \\ (j>i)}}^N e^{-(\alpha_i + \alpha_j) a_{ij}^+ - (\beta_i + \beta_j) a_{ij}^-} = \prod_{i=1}^N \prod_{\substack{j=1 \\ (j>i)}}^N \sum_{a_{ij} = -1, 0, 1} e^{-(\alpha_i + \alpha_j) a_{ij}^+ - (\beta_i + \beta_j) a_{ij}^-} = \prod_{i=1}^N \prod_{\substack{j=1 \\ (j>i)}}^N (1 + e^{-(\alpha_i + \alpha_j)} + e^{-(\beta_i + \beta_j)}) \tag{87}
\end{aligned}$$

and induces the expression

$$P_{\text{SCM}}(\mathbf{A}) = \frac{e^{-\sum_{i=1}^N [\alpha_i k_i^+(\mathbf{A}) + \beta_i k_i^-(\mathbf{A})]}}{\prod_{i=1}^N \prod_{\substack{j=1 \\ (j>i)}}^N (1 + e^{-(\alpha_i + \alpha_j)} + e^{-(\beta_i + \beta_j)})} \equiv \frac{\prod_{i=1}^N x_i^{k_i^+(\mathbf{A})} y_i^{k_i^-(\mathbf{A})}}{\prod_{i=1}^N \prod_{\substack{j=1 \\ (j>i)}}^N (1 + x_i x_j + y_i y_j)} \equiv \prod_{i=1}^N \prod_{\substack{j=1 \\ (j>i)}}^N (p_{ij}^-)^{a_{ij}^-} (p_{ij}^0)^{a_{ij}^0} (p_{ij}^+)^{a_{ij}^+} \quad (88)$$

having posed $p_{ij}^- \equiv \frac{e^{-(\beta_i + \beta_j)}}{1 + e^{-(\alpha_i + \alpha_j)} + e^{-(\beta_i + \beta_j)}} \equiv \frac{y_i y_j}{1 + x_i x_j + y_i y_j}$, $p_{ij}^0 \equiv \frac{1}{1 + e^{-(\alpha_i + \alpha_j)} + e^{-(\beta_i + \beta_j)}} \equiv \frac{1}{1 + x_i x_j + y_i y_j}$ and $p_{ij}^+ \equiv \frac{e^{-(\alpha_i + \alpha_j)}}{1 + e^{-(\alpha_i + \alpha_j)} + e^{-(\beta_i + \beta_j)}} \equiv \frac{x_i x_j}{1 + x_i x_j + y_i y_j}$, where p_{ij}^+ is the probability that nodes i and j are linked by a positive edge, p_{ij}^- is the probability that nodes i and j are linked by a negative edge and p_{ij}^0 is the probability that nodes i and j are no linked at all. Hence, according to the SCM, the generic entry of a signed network is a random variable following a generalized Bernoulli distribution, i.e. obeying the finite scheme

$$a_{ij} \sim \begin{pmatrix} -1 & 0 & +1 \\ p_{ij}^- & p_{ij}^0 & p_{ij}^+ \end{pmatrix} \quad \forall i < j; \quad (89)$$

as a consequence, any network belonging to \mathbb{A} is a collection of independent random variables, each one obeying the finite scheme

$$\mathbf{A} \sim \bigotimes \begin{pmatrix} -1 & 0 & +1 \\ p_{ij}^- & p_{ij}^0 & p_{ij}^+ \end{pmatrix} \quad (90)$$

i.e. the directed product of the $\frac{N(N-1)}{2} = \binom{N}{2}$ finite schemes above.

In the case of the SCM, L^+ is a random variable obeying the Poisson-Binomial distribution that we indicate as $\text{PoisBin}\left(\binom{N}{2}, \{p_{ij}^+\}_{i,j=1}^N\right)$; analogously, $L^- \sim \text{PoisBin}\left(\binom{N}{2}, \{p_{ij}^-\}_{i,j=1}^N\right)$. Similarly, k_i^+ is a random variable obeying the Poisson-Binomial distribution that we indicate as $\text{PoisBin}(N-1, \{p_{ij}^+\}_{j=1}^N)$; analogously, $k_i^- \sim \text{PoisBin}(N-1, \{p_{ij}^-\}_{j=1}^N)$. Hence, the total number of expected, positive links reads $\langle L^+ \rangle = \sum_{i=1}^N \sum_{\substack{j=1 \\ (j>i)}}^N p_{ij}^+$ while the total number of expected, negative links reads $\langle L^- \rangle = \sum_{i=1}^N \sum_{\substack{j=1 \\ (j>i)}}^N p_{ij}^-$; analogously, $\langle k_i^+ \rangle = \sum_{\substack{j=1 \\ (j \neq i)}}^N p_{ij}^+$ and $\langle k_i^- \rangle = \sum_{\substack{j=1 \\ (j \neq i)}}^N p_{ij}^-$.

In order to determine the parameters that define the SCM, let us maximize the likelihood function

$$\begin{aligned} \mathcal{L}_{\text{SCM}}(\{x_i\}_{i=1}^N, \{y_i\}_{i=1}^N) &\equiv \ln P_{\text{SCM}}(\mathbf{A}^* | \{x_i\}_{i=1}^N, \{y_i\}_{i=1}^N) \\ &= \sum_{i=1}^N k_i^+(\mathbf{A}^*) \ln(x_i) + \sum_{i=1}^N k_i^-(\mathbf{A}^*) \ln(y_i) - \sum_{i=1}^N \sum_{\substack{j=1 \\ (j>i)}}^N \ln(1 + x_i x_j + y_i y_j) \end{aligned} \quad (91)$$

with respect to x_i and y_i , $\forall i$. Upon doing so, we obtain the system of equations

$$\frac{\partial \mathcal{L}_{\text{SCM}}(\{x_i\}_{i=1}^N, \{y_i\}_{i=1}^N)}{\partial x_i} = \frac{k_i^+(\mathbf{A}^*)}{x_i} - \sum_{\substack{j=1 \\ (j \neq i)}}^N \frac{x_j}{1 + x_i x_j + y_i y_j} \quad \forall i, \quad (92)$$

$$\frac{\partial \mathcal{L}_{\text{SCM}}(\{x_i\}_{i=1}^N, \{y_i\}_{i=1}^N)}{\partial y_i} = \frac{k_i^-(\mathbf{A}^*)}{y_i} - \sum_{\substack{j=1 \\ (j \neq i)}}^N \frac{y_j}{1 + x_i x_j + y_i y_j} \quad \forall i; \quad (93)$$

equating them to zero leads us to find

$$k_i^+(\mathbf{A}^*) = \sum_{\substack{j=1 \\ (j \neq i)}}^N \frac{x_i x_j}{1 + x_i x_j + y_i y_j} = \sum_{\substack{j=1 \\ (j \neq i)}}^N p_{ij}^+ = \langle k_i^+ \rangle \quad \forall i, \quad (94)$$

$$k_i^-(\mathbf{A}^*) = \sum_{\substack{j=1 \\ (j \neq i)}}^N \frac{y_i y_j}{1 + x_i x_j + y_i y_j} = \sum_{\substack{j=1 \\ (j \neq i)}}^N p_{ij}^- = \langle k_i^- \rangle \quad \forall i. \quad (95)$$

Although the system above can be solved only numerically, particular conditions exist under which the equations constituting it can be approximated and solved explicitly. They are collectively named ‘sparse-case’ approximation of the SCM and hold true whenever $x_i \ll 1$ and $y_i \ll 1$, $\forall i$. In this case, one can pose $p_{ij}^+ \simeq x_i x_j$ and $p_{ij}^- \simeq y_i y_j$, $\forall i < j$, which allow the equations above to be simplified as follows

$$k_i^+(\mathbf{A}^*) \simeq \sum_{\substack{j=1 \\ (j \neq i)}}^N x_i x_j \quad \forall i, \quad (96)$$

$$k_i^-(\mathbf{A}^*) \simeq \sum_{\substack{j=1 \\ (j \neq i)}}^N y_i y_j \quad \forall i; \quad (97)$$

the latter ones induce the expressions $x_i = \frac{k_i^+(\mathbf{A}^*)}{\sum_{j=1}^N x_j} = \frac{k_i^+(\mathbf{A}^*)}{\sqrt{2L^+(\mathbf{A}^*)}}$ and $y_i = \frac{k_i^-(\mathbf{A}^*)}{\sum_{j=1}^N y_j} = \frac{k_i^-(\mathbf{A}^*)}{\sqrt{2L^-(\mathbf{A}^*)}}$, $\forall i$, allowing us to find

$$p_{ij}^+ \simeq \frac{k_i^+(\mathbf{A}^*) k_j^+(\mathbf{A}^*)}{2L^+(\mathbf{A}^*)}, \quad (98)$$

$$p_{ij}^- \simeq \frac{k_i^-(\mathbf{A}^*) k_j^-(\mathbf{A}^*)}{2L^-(\mathbf{A}^*)}. \quad (99)$$

The system of equations above is also known with the name of Signed Chung-Lu Model (SCLM).

Signed Configuration Model with fixed topology

Let us, again, consider the properties $\{k_i^+(\mathbf{A})\}_{i=1}^N$ and $\{k_i^-(\mathbf{A})\}_{i=1}^N$, to be satisfied by keeping a network topology fixed. As usual, we will indicate the adopted topology as the one induced by the matrix \mathbf{A}^* . The Hamiltonian describing such a problem still reads

$$H(\mathbf{A}) = \sum_{i=1}^N [\alpha_i k_i^+(\mathbf{A}) + \beta_i k_i^-(\mathbf{A})] \quad (100)$$

but induces a partition function reading

$$\begin{aligned} Z &= \sum_{\substack{\mathbf{A} \in \mathbb{A} \\ (|\mathbf{A}| = |\mathbf{A}^*|)}} e^{-H(\mathbf{A})} = \sum_{\substack{\mathbf{A} \in \mathbb{A} \\ (|\mathbf{A}| = |\mathbf{A}^*|)}} e^{-\sum_{i=1}^N [\alpha_i k_i^+(\mathbf{A}) + \beta_i k_i^-(\mathbf{A})]} = \sum_{\substack{\mathbf{A} \in \mathbb{A} \\ (|\mathbf{A}| = |\mathbf{A}^*|)}} e^{-\sum_{i=1}^N \sum_{j(>i)=1}^N [(\alpha_i + \alpha_j) a_{ij}^+ + (\beta_i + \beta_j) a_{ij}^-]} \\ &= \sum_{\substack{\mathbf{A} \in \mathbb{A} \\ (|\mathbf{A}| = |\mathbf{A}^*|)}} \prod_{i=1}^N \prod_{\substack{j=1 \\ (j > i)}}^N e^{-(\alpha_i + \alpha_j) a_{ij}^+ - (\beta_i + \beta_j) a_{ij}^-} = \prod_{i=1}^N \prod_{\substack{j=1 \\ (j > i)}}^N \left(\sum_{a_{ij} = -1, 1} e^{-(\alpha_i + \alpha_j) a_{ij}^+ - (\beta_i + \beta_j) a_{ij}^-} \right)^{|a_{ij}^*|} \\ &= \prod_{i=1}^N \prod_{\substack{j=1 \\ (j > i)}}^N \left(e^{-(\alpha_i + \alpha_j)} + e^{-(\beta_i + \beta_j)} \right)^{|a_{ij}^*|} \end{aligned} \quad (101)$$

which, in turn, induces the expression

$$\begin{aligned}
P_{\text{SCM-FT}}(\mathbf{A}) &= \frac{e^{-\sum_{i=1}^N [\alpha_i k_i^+(\mathbf{A}) + \beta_i k_i^-(\mathbf{A})]}}{\prod_{i=1}^N \prod_{\substack{j=1 \\ (j>i)}}^N (e^{-(\alpha_i + \alpha_j)} + e^{-(\beta_i + \beta_j)})^{|a_{ij}^*|}} \equiv \frac{\prod_{i=1}^N x_i^{k_i^+(\mathbf{A})} y_i^{k_i^-(\mathbf{A})}}{\prod_{i=1}^N \prod_{\substack{j=1 \\ (j>i)}}^N (x_i x_j + y_i y_j)^{|a_{ij}^*|}} \\
&\equiv \prod_{i=1}^N \prod_{\substack{j=1 \\ (j>i)}}^N \left[(p_{ij}^-)^{a_{ij}^-} (p_{ij}^+)^{a_{ij}^+} \right]^{|a_{ij}^*|} = \prod_{i=1}^N \prod_{\substack{j=1 \\ (j>i)}}^N (p_{ij}^-)^{a_{ij}^-} (p_{ij}^+)^{a_{ij}^+}
\end{aligned} \tag{102}$$

having posed $p_{ij}^- \equiv \frac{e^{-(\beta_i + \beta_j)}}{e^{-(\alpha_i + \alpha_j)} + e^{-(\beta_i + \beta_j)}} \equiv \frac{y_i y_j}{x_i x_j + y_i y_j}$ and $p_{ij}^+ \equiv \frac{e^{-(\alpha_i + \alpha_j)}}{e^{-(\alpha_i + \alpha_j)} + e^{-(\beta_i + \beta_j)}} \equiv \frac{x_i x_j}{x_i x_j + y_i y_j}$ where p_{ij}^+ is the probability that nodes i and j are linked by a positive edge and p_{ij}^- is the probability that nodes i and j are linked by a negative edge. Hence, according to the SCM-FT, the generic entry of a signed network satisfying $|a_{ij}| = |a_{ij}^*| = 1$ is a random variable following a Bernoulli distribution, i.e. obeying the finite scheme

$$a_{ij} \sim \begin{pmatrix} -1 & +1 \\ p_{ij}^- & p_{ij}^+ \end{pmatrix} \quad \forall i < j \mid |a_{ij}^*| = 1. \tag{103}$$

In the case of the SCM-FT, L^+ is a random variable obeying the Poisson-Binomial distribution that we indicate as $\text{PoissBin}(L, \{p_{ij}^+\}_{i,j=1}^N)$; analogously, $L^- \sim \text{PoissBin}(L, \{p_{ij}^-\}_{i,j=1}^N)$. Similarly, k_i^+ is a random variable obeying the Poisson-Binomial distribution that we indicate as $\text{PoissBin}(k_i, \{p_{ij}^+\}_{j=1}^N)$; analogously, $k_i^- \sim \text{PoissBin}(k_i, \{p_{ij}^-\}_{j=1}^N)$. Hence, the total number of expected, positive links reads $\langle L^+ \rangle = \sum_{i=1}^N \sum_{j(>i)=1}^N |a_{ij}^*| p_{ij}^+$ while the total number of expected, negative links reads $\langle L^- \rangle = \sum_{i=1}^N \sum_{j(>i)=1}^N |a_{ij}^*| p_{ij}^-$; analogously, $\langle k_i^+ \rangle = \sum_{j(\neq i)=1}^N |a_{ij}^*| p_{ij}^+$ and $\langle k_i^- \rangle = \sum_{j(\neq i)=1}^N |a_{ij}^*| p_{ij}^-$.

In order to determine the parameters that define the SCM-FT, let us maximize the likelihood function

$$\begin{aligned}
\mathcal{L}_{\text{SCM-FT}}(\{x_i\}_{i=1}^N, \{y_i\}_{i=1}^N) &\equiv \ln P_{\text{SCM-FT}}(\mathbf{A}^* | \{x_i\}_{i=1}^N, \{y_i\}_{i=1}^N) \\
&= \sum_{i=1}^N k_i^+(\mathbf{A}^*) \ln(x_i) + \sum_{i=1}^N k_i^-(\mathbf{A}^*) \ln(y_i) - \sum_{i=1}^N \sum_{\substack{j=1 \\ (j>i)}}^N |a_{ij}^*| \ln(x_i x_j + y_i y_j)
\end{aligned} \tag{104}$$

with respect to x_i and y_i , $\forall i$. Upon doing so, we obtain the system of equations

$$\frac{\partial \mathcal{L}_{\text{SCM-FT}}(\{x_i\}_{i=1}^N, \{y_i\}_{i=1}^N)}{\partial x_i} = \frac{k_i^+(\mathbf{A}^*)}{x_i} - \sum_{\substack{j=1 \\ (j \neq i)}}^N |a_{ij}^*| \frac{x_j}{x_i x_j + y_i y_j} \quad \forall i, \tag{105}$$

$$\frac{\partial \mathcal{L}_{\text{SCM-FT}}(\{x_i\}_{i=1}^N, \{y_i\}_{i=1}^N)}{\partial y_i} = \frac{k_i^-(\mathbf{A}^*)}{y_i} - \sum_{\substack{j=1 \\ (j \neq i)}}^N |a_{ij}^*| \frac{y_j}{x_i x_j + y_i y_j} \quad \forall i; \tag{106}$$

equating them to zero leads us to find

$$k_i^+(\mathbf{A}^*) = \sum_{\substack{j=1 \\ (j \neq i)}}^N |a_{ij}^*| \frac{x_i x_j}{x_i x_j + y_i y_j} = \sum_{\substack{j=1 \\ (j \neq i)}}^N |a_{ij}^*| p_{ij}^+ = \langle k_i^+ \rangle \quad \forall i, \tag{107}$$

$$k_i^-(\mathbf{A}^*) = \sum_{\substack{j=1 \\ (j \neq i)}}^N |a_{ij}^*| \frac{y_i y_j}{x_i x_j + y_i y_j} = \sum_{\substack{j=1 \\ (j \neq i)}}^N |a_{ij}^*| p_{ij}^- = \langle k_i^- \rangle \quad \forall i. \tag{108}$$

The system above can be solved only numerically.

Signed Configuration Model: free VS fixed topology

In order to clarify the relationship between the SCM and the SCM-FT, let us write

$$\begin{aligned}
P_{\text{SCM}}(\mathbf{A}) &= P_{\text{FM}}(\mathbf{A}) \cdot \frac{P_{\text{SCM}}(\mathbf{A})}{P_{\text{FM}}(\mathbf{A})} \\
&= \prod_{i=1}^N \prod_{\substack{j=1 \\ (j>i)}}^N p_{ij}^{a_{ij}} (1-p_{ij})^{1-a_{ij}} \cdot \frac{\prod_{i=1}^N \prod_{\substack{j=1 \\ (j>i)}}^N (p_{ij}^-)^{a_{ij}^-} (p_{ij}^+)^{a_{ij}^+} (1-p_{ij}^- - p_{ij}^+)^{1-a_{ij}^- - a_{ij}^+}}{\prod_{i=1}^N \prod_{\substack{j=1 \\ (j>i)}}^N p_{ij}^{a_{ij}} (1-p_{ij})^{1-a_{ij}}} \\
&= \prod_{i=1}^N \prod_{\substack{j=1 \\ (j>i)}}^N p_{ij}^{a_{ij}} (1-p_{ij})^{1-a_{ij}} \cdot \frac{\prod_{i=1}^N \prod_{\substack{j=1 \\ (j>i)}}^N (p_{ij}^-)^{a_{ij}^-} (p_{ij}^+)^{a_{ij}^+} (1-p_{ij}^- - p_{ij}^+)^{1-a_{ij}^- - a_{ij}^+}}{\prod_{i=1}^N \prod_{\substack{j=1 \\ (j>i)}}^N p_{ij}^{a_{ij}^- + a_{ij}^+} (1-p_{ij})^{1-a_{ij}^- - a_{ij}^+}} \\
&= \prod_{i=1}^N \prod_{\substack{j=1 \\ (j>i)}}^N p_{ij}^{a_{ij}} (1-p_{ij})^{1-a_{ij}} \cdot \prod_{i=1}^N \prod_{\substack{j=1 \\ (j>i)}}^N \left(\frac{p_{ij}^-}{p_{ij}} \right)^{a_{ij}^-} \left(\frac{p_{ij}^+}{p_{ij}} \right)^{a_{ij}^+} \left(\frac{1-p_{ij}^- - p_{ij}^+}{1-p_{ij}} \right)^{1-a_{ij}^- - a_{ij}^+} \quad (109)
\end{aligned}$$

where $P_{\text{FM}}(\mathbf{A})$ indicates the probability distribution of a generic, factorizable (null) model. Upon requiring $p_{ij} \equiv p_{ij}^- + p_{ij}^+$, we turn the FM into a Configuration Model (CM) whose coefficients are ‘induced’ by the ones of the SCM (in fact, $k_i(\mathbf{A}^*) = k_i^-(\mathbf{A}^*) + k_i^+(\mathbf{A}^*) = \sum_{j(\neq i)=1}^N p_{ij}^- + \sum_{j(\neq i)=1}^N p_{ij}^+ = \sum_{j(\neq i)=1}^N [p_{ij}^- + p_{ij}^+] = \sum_{j(\neq i)=1}^N p_{ij}$) and obtain

$$P_{\text{SCM}}(\mathbf{A}) = \prod_{i=1}^N \prod_{\substack{j=1 \\ (j>i)}}^N p_{ij}^{a_{ij}} (1-p_{ij})^{1-a_{ij}} \cdot \prod_{i=1}^N \prod_{\substack{j=1 \\ (j>i)}}^N \left(\frac{p_{ij}^-}{p_{ij}} \right)^{a_{ij}^-} \left(\frac{p_{ij}^+}{p_{ij}} \right)^{a_{ij}^+} \quad (110)$$

i.e. an expression that is the product of two probability distributions. Let us start from the second one, whose parameters read

$$\frac{p_{ij}^-}{p_{ij}} = \frac{p_{ij}^-}{p_{ij}^- + p_{ij}^+} = \frac{y_i y_j / (1 + x_i x_j + y_i y_j)}{x_i x_j / (1 + x_i x_j + y_i y_j) + y_i y_j / (1 + x_i x_j + y_i y_j)} = \frac{y_i y_j}{x_i x_j + y_i y_j}, \quad (111)$$

$$\frac{p_{ij}^+}{p_{ij}} = \frac{p_{ij}^+}{p_{ij}^- + p_{ij}^+} = \frac{x_i x_j / (1 + x_i x_j + y_i y_j)}{x_i x_j / (1 + x_i x_j + y_i y_j) + y_i y_j / (1 + x_i x_j + y_i y_j)} = \frac{x_i x_j}{x_i x_j + y_i y_j} \quad (112)$$

hence inducing the probability distribution of the SCM-FT, beside keeping the intuitive meaning made explicit by the expressions $p_{ij}^-/p_{ij} = P(\text{‘link -’} | \text{‘link’})$ and $p_{ij}^+/p_{ij} = P(\text{‘link +’} | \text{‘link’})$. The first one, on the other hand, can be identified with the probability distribution of the ‘induced’ CM:

$$\begin{aligned}
p_{ij} &= p_{ij}^- + p_{ij}^+ = \frac{y_i y_j}{1 + x_i x_j + y_i y_j} + \frac{x_i x_j}{1 + x_i x_j + y_i y_j} = \frac{y_i y_j + x_i x_j}{1 + x_i x_j + y_i y_j} \\
&= \frac{\mathbf{z}_i \cdot \mathbf{z}_j}{1 + \mathbf{z}_i \cdot \mathbf{z}_j} = \frac{|\mathbf{z}_i| |\mathbf{z}_j| \cos \phi_{ij}}{1 + |\mathbf{z}_i| |\mathbf{z}_j| \cos \phi_{ij}} = \frac{\sqrt{(x_i^2 + y_i^2)} \cos \phi_{ij} \cdot \sqrt{(x_j^2 + y_j^2)} \cos \phi_{ij}}{1 + \sqrt{(x_i^2 + y_i^2)} \cos \phi_{ij} \cdot \sqrt{(x_j^2 + y_j^2)} \cos \phi_{ij}} \equiv \frac{z_i z_j \cos \phi_{ij}}{1 + z_i z_j \cos \phi_{ij}} \quad (113)
\end{aligned}$$

where $\mathbf{z}_i \equiv (x_i, y_i)$ is the vector of fitnesses of node i , $z_i \equiv |\mathbf{z}_i| = \sqrt{(x_i^2 + y_i^2)}$ is its modulus and $\cos \phi_{ij}$ is the cosine of the angle between vectors \mathbf{z}_i and \mathbf{z}_j . As a consequence, we can write

$$P_{\text{SCM}}(\mathbf{A}) = P_{\text{ICM}}(\mathbf{A}) \cdot P_{\text{SCM-FT}}(\mathbf{A}). \quad (114)$$

Notice that when $z_i = (x_i, 0)$ and $z_j = (x_j, 0)$, $\cos \phi_{ij} = 1$ and $p_{ij} = p_{ij}^+ = \frac{x_i x_j}{1+x_i x_j}$, i.e. the ‘induced’ CM reduces to the proper CM: in this case, in fact, the information about signs is ‘redundant’ as $k_i(\mathbf{A}^*) = k_i^+(\mathbf{A}^*)$ and $k_j(\mathbf{A}^*) = k_j^+(\mathbf{A}^*)$. On the other hand, when $z_i = (x_i, 0)$ and $z_j = (0, y_j)$, $\cos \phi_{ij} = 0$ and $p_{ij} = 0$, i.e. nodes i and j cannot be linked: in this case, in fact, $k_i(\mathbf{A}^*) = k_i^+(\mathbf{A}^*)$ but $k_j(\mathbf{A}^*) = k_j^-(\mathbf{A}^*)$, whence the impossibility of (consistently) attributing a sign to the edge between i and j .

APPENDIX D. NUMERICAL OPTIMIZATION OF LIKELIHOOD FUNCTIONS

In order to numerically solve the systems of equations defining the SCM and the SCM-FT, we can follow the guidelines provided in [40]: more specifically, we will adapt the iterative recipe provided there to our (binary, undirected, signed) setting. First, let us consider the SCM whose system of equations can be rewritten as

$$x_i = \frac{k_i^+(\mathbf{A}^*)}{\sum_{\substack{j=1 \\ (j \neq i)}}^N \frac{x_j}{1+x_i x_j + y_i y_j}} \implies x_i^{(n)} = \frac{k_i^+(\mathbf{A}^*)}{\sum_{\substack{j=1 \\ (j \neq i)}}^N \frac{x_j^{(n-1)}}{1+x_i^{(n-1)} x_j^{(n-1)} + y_i^{(n-1)} y_j^{(n-1)}}} \quad \forall i, \quad (115)$$

$$y_i = \frac{k_i^-(\mathbf{A}^*)}{\sum_{\substack{j=1 \\ (j \neq i)}}^N \frac{y_j}{1+x_i x_j + y_i y_j}} \implies y_i^{(n)} = \frac{k_i^-(\mathbf{A}^*)}{\sum_{\substack{j=1 \\ (j \neq i)}}^N \frac{y_j^{(n-1)}}{1+x_i^{(n-1)} x_j^{(n-1)} + y_i^{(n-1)} y_j^{(n-1)}}} \quad \forall i; \quad (116)$$

analogously, the system of equations defining the SCM-FT can be rewritten as

$$x_i = \frac{k_i^+(\mathbf{A}^*)}{\sum_{\substack{j=1 \\ (j \neq i)}}^N |a_{ij}^*| \frac{x_j}{x_i x_j + y_i y_j}} \implies x_i^{(n)} = \frac{k_i^+(\mathbf{A}^*)}{\sum_{\substack{j=1 \\ (j \neq i)}}^N |a_{ij}^*| \frac{x_j^{(n-1)}}{x_i^{(n-1)} x_j^{(n-1)} + y_i^{(n-1)} y_j^{(n-1)}}} \quad \forall i, \quad (117)$$

$$y_i = \frac{k_i^-(\mathbf{A}^*)}{\sum_{\substack{j=1 \\ (j \neq i)}}^N |a_{ij}^*| \frac{y_j}{x_i x_j + y_i y_j}} \implies y_i^{(n)} = \frac{k_i^-(\mathbf{A}^*)}{\sum_{\substack{j=1 \\ (j \neq i)}}^N |a_{ij}^*| \frac{y_j^{(n-1)}}{x_i^{(n-1)} x_j^{(n-1)} + y_i^{(n-1)} y_j^{(n-1)}}} \quad \forall i. \quad (118)$$

In order for each iterative recipe to converge, an appropriate vector of initial conditions need to be chosen; here, we have opted the following ones: $x_i = k_i^+(\mathbf{A}^*)/\sqrt{2L^+(\mathbf{A}^*)}$, $\forall i$ and $y_i = k_i^-(\mathbf{A}^*)/\sqrt{2L^-(\mathbf{A}^*)}$, $\forall i$. Besides, we have adopted two, different stopping criteria: the first one is a condition on the Euclidean norm of the vector of differences between the values of the parameters at subsequent iterations, i.e. $\|\Delta\theta\|_2 = \sqrt{\sum_{i=1}^N (\Delta\theta_i)^2} \leq 10^{-8}$; the second one is a condition on the maximum number of iterations of our iterative algorithm, set to 10^3 .

The accuracy of our method in estimating the constraints has been evaluated by computing the *maximum absolute error* (MAE), defined as

$$\text{MAE} = \max_i \{ |k_i^+(\mathbf{A}^*) - \langle k_i^+ \rangle|, |k_i^-(\mathbf{A}^*) - \langle k_i^- \rangle| \} \quad (119)$$

(i.e. as the infinite norm of the difference between the vector of the empirical values of the constraints and the vector of their expected values) and the *maximum relative error* (MRE), defined as

$$\text{MRE} = \max_i \left\{ \frac{|k_i^+(\mathbf{A}^*) - \langle k_i^+ \rangle|}{k_i^+(\mathbf{A}^*)}, \frac{|k_i^-(\mathbf{A}^*) - \langle k_i^- \rangle|}{k_i^-(\mathbf{A}^*)} \right\} \quad (120)$$

(i.e. as the infinite norm of the relative difference between the vector of the empirical values of the constraints and the vector of their expected values).

The following tables sum up the time employed by our algorithm to converge as well as its accuracy in reproducing the constraints defining the SCM and the SCM-FT on each network considered in the present contribution. Overall, our method is fast and accurate: the numerical errors never exceed $O(10^{-1})$ and the time employed to achieve such an accuracy never exceeds minutes. To be noticed that the time required by our algorithm to solve the SCM is usually smaller than that required to solve the SCM-FT - although such a difference rises with the size of the considered configuration.

						SCM			SCM-FT		
	N	L	L^+	L^-	c	MAE	MRE	Time (s)	MAE	MRE	Time (s)
CoW, 1946-49	60	360	319	41	$\simeq 2.0 \cdot 10^{-3}$	$\simeq 6.4 \cdot 10^{-2}$	$\simeq 1.4 \cdot 10^{-2}$	$\simeq 0.02$	$\simeq 7.1 \cdot 10^{-2}$	$\simeq 3.9 \cdot 10^{-3}$	$\simeq 0.01$
CoW, 1950-53	72	437	361	76	$\simeq 1.7 \cdot 10^{-3}$	$\simeq 7.6 \cdot 10^{-2}$	$\simeq 2.1 \cdot 10^{-2}$	$\simeq 0.02$	$\simeq 6.0 \cdot 10^{-2}$	$\simeq 3.2 \cdot 10^{-2}$	$\simeq 0.01$
CoW, 1954-57	80	492	418	74	$\simeq 1.5 \cdot 10^{-3}$	$\simeq 7.6 \cdot 10^{-2}$	$\simeq 2.2 \cdot 10^{-2}$	$\simeq 0.03$	$\simeq 8.3 \cdot 10^{-2}$	$\simeq 2.8 \cdot 10^{-2}$	$\simeq 0.02$
CoW, 1958-61	101	613	506	107	$\simeq 1.2 \cdot 10^{-3}$	$\simeq 8.5 \cdot 10^{-2}$	$\simeq 2.2 \cdot 10^{-2}$	$\simeq 0.04$	$\simeq 9.7 \cdot 10^{-2}$	$\simeq 2.9 \cdot 10^{-2}$	$\simeq 0.03$
CoW, 1962-65	109	642	540	102	$\simeq 1.1 \cdot 10^{-3}$	$\simeq 7.9 \cdot 10^{-2}$	$\simeq 1.9 \cdot 10^{-2}$	$\simeq 0.06$	$\simeq 9.8 \cdot 10^{-2}$	$\simeq 5.2 \cdot 10^{-2}$	$\simeq 0.03$
CoW, 1966-69	111	607	504	103	$\simeq 9.9 \cdot 10^{-4}$	$\simeq 6.9 \cdot 10^{-2}$	$\simeq 2.2 \cdot 10^{-2}$	$\simeq 0.05$	$\simeq 5.8 \cdot 10^{-2}$	$\simeq 5.8 \cdot 10^{-2}$	$\simeq 0.03$
CoW, 1970-73	111	677	595	82	$\simeq 1.1 \cdot 10^{-3}$	$\simeq 7.6 \cdot 10^{-2}$	$\simeq 2.0 \cdot 10^{-2}$	$\simeq 0.05$	$\simeq 7.2 \cdot 10^{-2}$	$\simeq 7.2 \cdot 10^{-2}$	$\simeq 0.03$
CoW, 1974-77	123	813	699	114	$\simeq 1.1 \cdot 10^{-3}$	$\simeq 8.8 \cdot 10^{-2}$	$\simeq 2.3 \cdot 10^{-2}$	$\simeq 0.06$	$\simeq 7.2 \cdot 10^{-2}$	$\simeq 3.1 \cdot 10^{-2}$	$\simeq 0.04$
CoW, 1978-81	134	999	907	92	$\simeq 1.1 \cdot 10^{-3}$	$\simeq 8.4 \cdot 10^{-2}$	$\simeq 2.3 \cdot 10^{-2}$	$\simeq 0.08$	$\simeq 6.5 \cdot 10^{-2}$	$\simeq 3.5 \cdot 10^{-2}$	$\simeq 0.06$
CoW, 1982-85	134	1042	935	107	$\simeq 1.1 \cdot 10^{-4}$	$\simeq 9.8 \cdot 10^{-2}$	$\simeq 2.3 \cdot 10^{-2}$	$\simeq 0.07$	$\simeq 8.2 \cdot 10^{-2}$	$\simeq 2.8 \cdot 10^{-2}$	$\simeq 0.05$
CoW, 1986-89	139	1079	989	90	$\simeq 1.1 \cdot 10^{-4}$	$\simeq 9.6 \cdot 10^{-2}$	$\simeq 2.6 \cdot 10^{-2}$	$\simeq 0.08$	$\simeq 8.9 \cdot 10^{-2}$	$\simeq 3.4 \cdot 10^{-2}$	$\simeq 0.06$
CoW, 1990-93	151	1286	1160	126	$\simeq 1.1 \cdot 10^{-4}$	$\simeq 9.8 \cdot 10^{-2}$	$\simeq 2.7 \cdot 10^{-2}$	$\simeq 0.12$	$\simeq 9.0 \cdot 10^{-2}$	$\simeq 3.1 \cdot 10^{-2}$	$\simeq 0.07$
CoW, 1994-97	143	1220	1099	121	$\simeq 1.2 \cdot 10^{-4}$	$\simeq 9.8 \cdot 10^{-2}$	$\simeq 2.8 \cdot 10^{-2}$	$\simeq 0.08$	$\simeq 5.3 \cdot 10^{-2}$	$\simeq 2.1 \cdot 10^{-2}$	$\simeq 0.06$

TABLE II: Performance of the fixed-point algorithm to solve the systems of equations defining the SCM and the SCM-FT on the snapshots of the CoW dataset.

						SCM			SCM-FT		
	N	L	L^+	L^-	c	MAE	MRE	Time (s)	MAE	MRE	Time (s)
MMOG, Day 10	1312	3791	3725	66	$\simeq 4.4 \cdot 10^{-3}$	$\simeq 1.2 \cdot 10^{-1}$	$\simeq 2.1 \cdot 10^{-2}$	$\simeq 7$	$\simeq 1.7 \cdot 10^{-2}$	$\simeq 1.0 \cdot 10^{-2}$	$\simeq 5$
MMOG, Day 20	1924	7032	6050	982	$\simeq 3.8 \cdot 10^{-3}$	$\simeq 1.4 \cdot 10^{-1}$	$\simeq 2.6 \cdot 10^{-2}$	$\simeq 9$	$\simeq 3.1 \cdot 10^{-2}$	$\simeq 1.5 \cdot 10^{-2}$	$\simeq 21$
MMOG, Day 30	2261	9046	7371	1675	$\simeq 3.5 \cdot 10^{-3}$	$\simeq 2.0 \cdot 10^{-1}$	$\simeq 3.1 \cdot 10^{-2}$	$\simeq 10$	$\simeq 6.5 \cdot 10^{-2}$	$\simeq 2.3 \cdot 10^{-2}$	$\simeq 34$
MMOG, Day 40	2544	11372	8403	2969	$\simeq 3.5 \cdot 10^{-3}$	$\simeq 2.0 \cdot 10^{-1}$	$\simeq 3.2 \cdot 10^{-2}$	$\simeq 12$	$\simeq 8.4 \cdot 10^{-2}$	$\simeq 2.2 \cdot 10^{-2}$	$\simeq 35$
MMOG, Day 50	2714	13228	9110	4118	$\simeq 3.6 \cdot 10^{-3}$	$\simeq 1.9 \cdot 10^{-1}$	$\simeq 3.3 \cdot 10^{-2}$	$\simeq 14$	$\simeq 1.2 \cdot 10^{-1}$	$\simeq 4.2 \cdot 10^{-2}$	$\simeq 54$
MMOG, Day 60	2923	13909	9711	4198	$\simeq 3.3 \cdot 10^{-3}$	$\simeq 2.0 \cdot 10^{-1}$	$\simeq 3.0 \cdot 10^{-2}$	$\simeq 18$	$\simeq 1.1 \cdot 10^{-1}$	$\simeq 3.8 \cdot 10^{-2}$	$\simeq 80$
MMOG, Day 70	3068	14963	10151	4812	$\simeq 3.2 \cdot 10^{-3}$	$\simeq 2.2 \cdot 10^{-1}$	$\simeq 3.2 \cdot 10^{-2}$	$\simeq 19$	$\simeq 9.1 \cdot 10^{-2}$	$\simeq 2.8 \cdot 10^{-2}$	$\simeq 85$
MMOG, Day 80	3221	16318	10745	5573	$\simeq 3.2 \cdot 10^{-3}$	$\simeq 1.9 \cdot 10^{-1}$	$\simeq 3.0 \cdot 10^{-2}$	$\simeq 22$	$\simeq 1.1 \cdot 10^{-1}$	$\simeq 5.2 \cdot 10^{-2}$	$\simeq 109$
MMOG, Day 90	3363	17664	11342	6322	$\simeq 3.1 \cdot 10^{-3}$	$\simeq 2.0 \cdot 10^{-1}$	$\simeq 3.4 \cdot 10^{-2}$	$\simeq 25$	$\simeq 1.3 \cdot 10^{-1}$	$\simeq 4.5 \cdot 10^{-2}$	$\simeq 120$
MMOG, Day 100	3523	19008	11915	7093	$\simeq 3.1 \cdot 10^{-3}$	$\simeq 2.1 \cdot 10^{-1}$	$\simeq 3.2 \cdot 10^{-2}$	$\simeq 27$	$\simeq 1.1 \cdot 10^{-1}$	$\simeq 4.7 \cdot 10^{-2}$	$\simeq 138$

TABLE III: Performance of the fixed-point algorithm to solve the systems of equations defining the SCM and the SCM-FT on the snapshots of the MMOG dataset.

						SCM			SCM-FT		
	N	L	L^+	L^-	c	MAE	MRE	Time (s)	MAE	MRE	Time (s)
N.G.H. Tribes	16	58	29	29	$\simeq 0.48$	$\simeq 3.2 \cdot 10^{-2}$	$\simeq 1.1 \cdot 10^{-2}$	$\simeq 0.005$	$\simeq 2.7 \cdot 10^{-2}$	$\simeq 1.1 \cdot 10^{-2}$	$\simeq 0.0004$
Monastery	18	49	37	12	$\simeq 3.2 \cdot 10^{-1}$	$\simeq 2.4 \cdot 10^{-2}$	$\simeq 1.4 \cdot 10^{-2}$	$\simeq 0.006$	$\simeq 1.2 \cdot 10^{-2}$	$\simeq 9.3 \cdot 10^{-3}$	$\simeq 0.006$
Senate US	100	2461	1414	1047	$\simeq 4.9 \cdot 10^{-1}$	$\simeq 1.0 \cdot 10^{-1}$	$\simeq 1.1 \cdot 10^{-2}$	$\simeq 0.06$	$\simeq 5.9 \cdot 10^{-2}$	$\simeq 1.0 \cdot 10^{-2}$	$\simeq 0.12$
EGFR	313	755	499	256	$\simeq 1.5 \cdot 10^{-2}$	$\simeq 5.8 \cdot 10^{-2}$	$\simeq 2.1 \cdot 10^{-2}$	$\simeq 0.54$	$\simeq 3.8 \cdot 10^{-2}$	$\simeq 1.1 \cdot 10^{-2}$	$\simeq 0.35$
Macrophage	660	1397	931	466	$\simeq 6.4 \cdot 10^{-3}$	$\simeq 8.1 \cdot 10^{-2}$	$\simeq 2.1 \cdot 10^{-2}$	$\simeq 2$	$\simeq 2.6 \cdot 10^{-2}$	$\simeq 1.5 \cdot 10^{-2}$	$\simeq 1.8$
E. Coli	1376	3150	1848	1302	$\simeq 3.3 \cdot 10^{-3}$	$\simeq 1.9 \cdot 10^{-1}$	$\simeq 2.2 \cdot 10^{-2}$	$\simeq 13$	$\simeq 1.3 \cdot 10^{-2}$	$\simeq 1.2 \cdot 10^{-2}$	$\simeq 10$
Bitcoin Alpha	3775	14120	12721	1399	$\simeq 1.9 \cdot 10^{-3}$	$\simeq 2.1 \cdot 10^{-1}$	$\simeq 3.1 \cdot 10^{-2}$	$\simeq 76$	$\simeq 5.5 \cdot 10^{-2}$	$\simeq 2.2 \cdot 10^{-2}$	$\simeq 138$
Bitcoin OTC	5875	21489	18230	3259	$\simeq 1.2 \cdot 10^{-3}$	$\simeq 2.5 \cdot 10^{-1}$	$\simeq 4.0 \cdot 10^{-2}$	$\simeq 24$	$\simeq 1.1 \cdot 10^{-1}$	$\simeq 3.5 \cdot 10^{-2}$	$\simeq 267$

TABLE IV: Performance of the fixed-point algorithm to solve the systems of equations defining the SCM and the SCM-FT on a bunch of real-world networks.

APPENDIX E. INSPECTING HIGHER-ORDER FRUSTRATION ON SIGNED NETWORKS

In order to inspect the behaviour of frustration at the mesoscopic level, we have considered the signed modularity, defined as

$$\begin{aligned}
Q &= \sum_{i=1}^N \sum_{\substack{j=1 \\ (j>i)}}^N [a_{ij}^* - \langle a_{ij} \rangle] \delta_{c_i c_j} \\
&= \sum_{i=1}^N \sum_{\substack{j=1 \\ (j>i)}}^N [(a_{ij}^+)^* - (a_{ij}^-)^* - \langle a_{ij}^+ \rangle + \langle a_{ij}^- \rangle] \delta_{c_i c_j} \\
&= \sum_{i=1}^N \sum_{\substack{j=1 \\ (j>i)}}^N (a_{ij}^+)^* \delta_{c_i c_j} - \sum_{i=1}^N \sum_{\substack{j=1 \\ (j>i)}}^N (a_{ij}^-)^* \delta_{c_i c_j} - \sum_{i=1}^N \sum_{\substack{j=1 \\ (j>i)}}^N \langle a_{ij}^+ \rangle \delta_{c_i c_j} + \sum_{i=1}^N \sum_{\substack{j=1 \\ (j>i)}}^N \langle a_{ij}^- \rangle \delta_{c_i c_j} \\
&= \sum_{i=1}^N \sum_{\substack{j=1 \\ (j>i)}}^N (a_{ij}^+)^* \delta_{c_i c_j} - \sum_{i=1}^N \sum_{\substack{j=1 \\ (j>i)}}^N (a_{ij}^-)^* \delta_{c_i c_j} - \sum_{i=1}^N \sum_{\substack{j=1 \\ (j>i)}}^N p_{ij}^+ \delta_{c_i c_j} + \sum_{i=1}^N \sum_{\substack{j=1 \\ (j>i)}}^N p_{ij}^- \delta_{c_i c_j} \\
&= L_{\bullet}^+ - L_{\bullet}^- - \langle L_{\bullet}^+ \rangle + \langle L_{\bullet}^- \rangle \\
&= L^+ - L_{\circ}^+ - L_{\bullet}^- - \langle L^+ - L_{\circ}^+ \rangle + \langle L_{\bullet}^- \rangle \\
&= -(L_{\circ}^+ + L_{\bullet}^-) + \langle L_{\circ}^+ + L_{\bullet}^- \rangle + L^+ - \langle L^+ \rangle \\
&= -[(L_{\circ}^+ + L_{\bullet}^-) - \langle L_{\circ}^+ + L_{\bullet}^- \rangle] + L^+ - \langle L^+ \rangle
\end{aligned} \tag{121}$$

where

$$L_{\bullet}^+ = \sum_{i=1}^N \sum_{\substack{j=1 \\ (j>i)}}^N (a_{ij}^+)^* \delta_{c_i c_j} = \sum_{i=1}^N \sum_{\substack{j=1 \\ (j>i)}}^N (a_{ij}^+)^* - \sum_{i=1}^N \sum_{\substack{j=1 \\ (j>i)}}^N (a_{ij}^+)^* (1 - \delta_{c_i c_j}) = L^+ - L_{\circ}^+ \tag{122}$$

and analogously for L_{\bullet}^- : since the total number of positive links is preserved under any null model considered here, we obtain $Q = -[(L_{\circ}^+ + L_{\bullet}^-) - \langle L_{\circ}^+ + L_{\bullet}^- \rangle]$; moreover, if we employ a null model that preserves a network topology, the stronger result $Q = -L \cdot (\text{HOFI} - \langle \text{HOFI} \rangle)$ holds true and, since $L > 0$, maximizing Q becomes equivalent at minimizing the HOFI (that coincides with the percentage of ‘misplaced’ links, i.e. the total number of positive links between communities, L_{\circ}^+ , plus the total number of negative links within communities, L_{\bullet}^- , divided by the total number of links, L). Such a definition aims at capturing the ‘philosophy’ behind the concept of frustration, introduced by Heider, rephrased by the structure theorem (stating that a signed network is balanced if and only if its nodes can be partitioned into two subsets with the links within them being positive and the links between them being negative) and extended by Davis, whose definition allows the number of subsets to be larger than two.

Intuitively, maximizing modularity amounts at placing the nodes connected by a positive link within the same modules and the nodes connected by a negative link within different modules. Indeed, under the assumption $0 \leq p_{ij}^- \leq p_{ij}^+ \leq 1$, one has that

$$a_{ij}^* - (p_{ij}^+ - p_{ij}^-) = \begin{cases} +[1 - (p_{ij}^+ - p_{ij}^-)] > 0, & \text{if } a_{ij}^* = +1 \\ -[1 + (p_{ij}^+ - p_{ij}^-)] < 0, & \text{if } a_{ij}^* = -1 \end{cases} \tag{123}$$

i.e. $\text{sgn}(a_{ij}^*[1 - (p_{ij}^+ - p_{ij}^-)]) = \text{sgn}(a_{ij}^*)$; hence, Q rises (decreases) if $\delta_{c_i c_j} = 1$, i.e. $c_i = c_j$, and $a_{ij}^* = +1$ ($\delta_{c_i c_j} = 1$ and $a_{ij}^* = -1$).

A frustration-based community detection algorithm where the number of blocks, say k , is fixed a priori, thus remains naturally defined (see below). Notice that our exercise is defined in such a way that the numerical value of the generic addendum $a_{ij}^* - (p_{ij}^+ - p_{ij}^-)$ is fixed, once and for all, by the choice of the benchmark to be solved: in other words, the definition of modularity does not change with the level of aggregation, being just recomputed (as any other score function) as the partition changes.

Algorithm 1: Pseudocode to partition nodes in order to maximize the signed modularity Q

```

1: function ModularityBasedCommunityDetection( $N, k, \mathbf{A}$ )
2:  $C \leftarrow$  array of length  $N$ , randomly initialized with  $k$  different integers  $1 \dots k$ ;
3:  $Q \leftarrow \text{UpdateSignedModularity}(N, \mathbf{A}, C)$ ;
4:  $E \leftarrow$  randomly sorted edges;
5: for  $(u, v) \in E$  do
6:    $C_0 \leftarrow C$ ;
7:    $Q_0 \leftarrow Q$ ;
8:   if  $C(u) \neq C(v)$  then
9:      $C_1 \leftarrow C$ ;
10:     $C_1(u) \leftarrow C(v)$ ;
11:     $Q_1 \leftarrow \text{UpdateSignedModularity}(N, \mathbf{A}, C_1)$ ;
12:     $C_2 \leftarrow C$ ;
13:     $C_2(v) \leftarrow C(u)$ ;
14:     $Q_2 \leftarrow \text{UpdateSignedModularity}(N, \mathbf{A}, C_2)$ ;
15:   else if  $C(u) = C(v)$  then
16:      $C_1 \leftarrow C$ ;
17:      $C_1(u) \leftarrow$  randomly sorted community different from  $C(v)$ ;
18:      $Q_1 \leftarrow \text{UpdateSignedModularity}(N, \mathbf{A}, C_1)$ ;
19:      $C_2 \leftarrow C$ ;
20:      $C_2(v) \leftarrow$  randomly sorted community different from  $C(u)$ ;
21:      $Q_2 \leftarrow \text{UpdateSignedModularity}(N, \mathbf{A}, C_2)$ ;
22:   end if
23:    $i \leftarrow \text{argmax}\{Q_0, Q_1, Q_2\}$ ;
24:    $C \leftarrow C_i$ ;
25:    $Q \leftarrow Q_i$ ;
26: end for

```

Algorithm 2: Pseudocode to update the signed modularity Q

```

1: function UpdateSignedModularity( $N, \mathbf{A}, C$ )
2:  $\mathbf{P}^+ \leftarrow$  matrix whose generic element is the probability that the corresponding nodes are linked by a +1;
3:  $\mathbf{P}^- \leftarrow$  matrix whose generic element is the probability that the corresponding nodes are linked by a -1;
4:  $Q \leftarrow 0$ ;
5: for  $(u, v) \in E$  do
6:   if  $C(u) = C(v)$  do
7:      $Q = Q + \mathbf{A}(u, v) - \mathbf{P}^+(u, v) + \mathbf{P}^-(u, v)$ ;
8:   end if
9: end for

```
